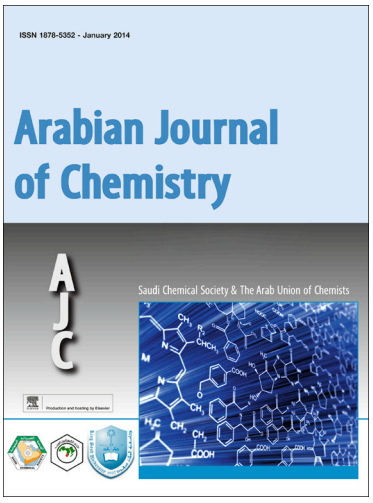


Original article

# Effect of L-threonine on Growth and Properties of Ammonium Dihydrogen Phosphate Crystal

J.H. Joshi, S. Kalainthan, D.K. Kanchan, M.J. Joshi, K.D. Parikh

PII: S1878-5352(17)30240-X
DOI: https://doi.org/10.1016/j.arabjc.2017.12.005
Reference: ARABJC 2197

To appear in: *Arabian Journal of Chemistry*

Received Date: 26 June 2017
Accepted Date: 5 December 2017

Please cite this article as: J.H. Joshi, S. Kalainthan, D.K. Kanchan, M.J. Joshi, K.D. Parikh, Effect of L-threonine on Growth and Properties of Ammonium Dihydrogen Phosphate Crystal, *Arabian Journal of Chemistry* (2017), doi: https://doi.org/10.1016/j.arabjc.2017.12.005

# Effect of L-threonine on Growth and Properties of Ammonium Dihydrogen Phosphate Crystal

J.H.Joshi[1*], S.Kalainthan[2], D.K.Kanchan[3], M.J.Joshi[1], K.D.Parikh[4**]

1. Department of Physics, Saurashtra University, Rajkot – 360 005 (India)

2. Centre for Crystal Growth, School of Advanced Sciences, VIT University, Vellore – 632014 (India)

3. Department of Physics, Faculty of Science, M.S.University of Baroda, Vadodara - 390 002 (India)

4. Department of Physics, Shri M.P.Shah Arts & Science College, Surendranagar – 363 001 (India)

Corresponding author email: *jaydeep_joshi1989@yahoo.com**ketandparikh@yahoo.co.in

**Abstract:** Ammonium dihydrogen phosphate (ADP) is an important nonlinear optical (NLO) material used for electro-optical applications and finds various NLO applications using Nd: YAG and Nd: YLF Lasers. The Amino acids have properties like molecular chirality and zwitter ionic nature helps to improve NLO properties of ADP. The pure and L-threonine doped ADP crystals are grown using slow solvent evaporation technique at room temperature. The Powder XRD spectra suggest tetragonal crystal system and slit shifting of peak. The FT-IR spectra verify the presence of various functional groups of pure and doped ADP crystals. The FT-Raman shows strong absorption peak at 922 $cm^{-1}$ due to asymmetric stretching of $PO_4^{3-}$ for all samples without shifting indicating the single phase nature of all samples. The photoluminescence study suggests the presence of defects in doped samples compared to the pure one due to increase of Stokes shift and vibrational energy relaxation phenomena. The presences of constituent elements are indentified using CHN analysis. The optical transmittance, energy band gap, skin depth, refractive index and extinction coefficient is study using UV-Visible spectroscopy and the dispersive behaviour of refractive index below absorption edge is study using Wemple-DiDomenico single oscillator model. The variation of capacitance and conductance is study using complex admittance spectroscopy. All the grown crystals possess negative photoconductivity. The second and third harmonic generation efficiency is increases nearly to double for L-threonine doped ADP crystals compared to pure Potassium dihydrogen phosphate (KDP). The laser damage threshold is measure for pure and doped ADP crystals.

**Keywords:** ADP, Vibrational energy relaxation, Stoke shift, Wemple-DiDomenico single oscillator model, Z-Scan, Complex admittance.

**Introduction:** Ammonium dihydrogen phosphate (ADP) belongs to a large number crystal family of $MH_2XO_4$ (Where, M = K, Na, $NH_4^+$, X = As, P). In ADP crystals, $NH_4^+$ can form N-H....O-P hydrogen bonding with $H_2PO_4$ [1]. It is used in short-wavelength laser technology, nonlinear and integrated optics as a bulk electro-optical devices, as a frequency converters of coherent radiation of high-power pico-second lasers, as an optical parametric oscillators for the infrared spectral region, and as an integral optical waveguides [2]. The Amino acids are bi-functional organic molecules that contain a carboxyl group (-COOH) as well as an amine group ($-NH_2$). In the solid state, amino acids have a protonated amino group ($NH_3^+$) and de-protonated carboxylic acid group ($COO^-$). The zwitter ionic nature exhibits peculiar physical and chemical properties in amino acid which makes them an ideal candidate for NLO applications [3]. Hence, the attempt have been made by researcher to study amino acids doped Potassium dihydrogen phosphate (KDP) [4-6] and ADP [7] crystals.

The L-threonine is an uncharged neutral amino acid and a useful compound for its nonlinear optical properties. It contains two asymmetric carbon atoms with a single carboxylate ($CO_2^-$) and amino ($NH_3^+$) group. It crystallizes in non-centrosymmetric $P2_12_12_1$ space group with 4 zwitter ionic molecules in the unit cell linked by a 3-dimensional network of hydrogen bonds of unequal strength [8]. Besides these, the L-threonine is having proton donor nature and having shorter side chain structure, such that it will easily combine with ADP lattice matrix and modifies the properties of pure ADP. By doping the L-threonine in ADP one can enhance the optical transparency, second and third order harmonic generation efficiency of pumped Nd:YAG lasers.

The present investigation devoted mainly toward linear and nonlinear optical performance of pure and L-threonine doped ADP crystals using Powder XRD, FT-IR, FT-Raman, photoluminescence, UV-Visible, SHG, Z-scan and laser threshold damage, also the present manuscript reflects the electrical counterpart of pure and doped ADP in terms of complex admittance spectroscopy.

The novelty of present work is that authors have study some of new phenomena which are rarely or not address by previous authors like Stoke shift, Wemple-DiDomenico single oscillator model for refractive index dispersion, Cohensive energy, Vibrational relaxation process, Complex admittance study, Defect oriented conduction mechanism like CBH and NSPT etc.

**Experimental Technique:** Presently, the slow solvent evaporation technique is employed for the growth of pure and different weight percentage (0.4 wt%, 0.6 wt% and 0.8 wt%) L-threonine doped ADP crystals. Initially, the solubility of ADP in distilled water is measured at room temperature and it is found to be 46 gram / 100 millilitres. The saturated solution is prepared by dissolving ADP gravimetrically in 400 millilitre triple distilled water and the solution is continuously stirred using magnetic stirrer until the saturation occurs. The pure ADP solution becomes saturated at 184 gram. The saturated solution then filtered using Watmann filter paper no.1 and the pure ADP solution is subdivided into four beakers, each of the beakers contains 100 millilitre of pure ADP solution. Here we keep one beaker as it is for the growth of pure ADP crystals, this beaker is shield properly with porous lid and on the lid 5-6 pin holes are made for the evaporation of water, and then it is keep in dust free atmosphere for the growth of crystal. Now, for the growth of L-threonine doped ADP crystals, the different amount of L-threonine (0.4 gram, 0.6 gram and 0.8 gram) is added into another three beakers one by one having pure ADP solution. Then again L-threonine contains ADP solutions are stirred for 4 hours to achieve homogeneous solution. After course of 8 hours the doped solutions are filtered again, shield with porous lid and put them in dust free atmosphere for the evaporation. The good quality and transparent crystals are harvested from all the solution after 20 days. The Figure 1 shows the grown crystals and the change of morphology clearly indicates the effect of dopant (L-threonine) on crystal growth of ADP.

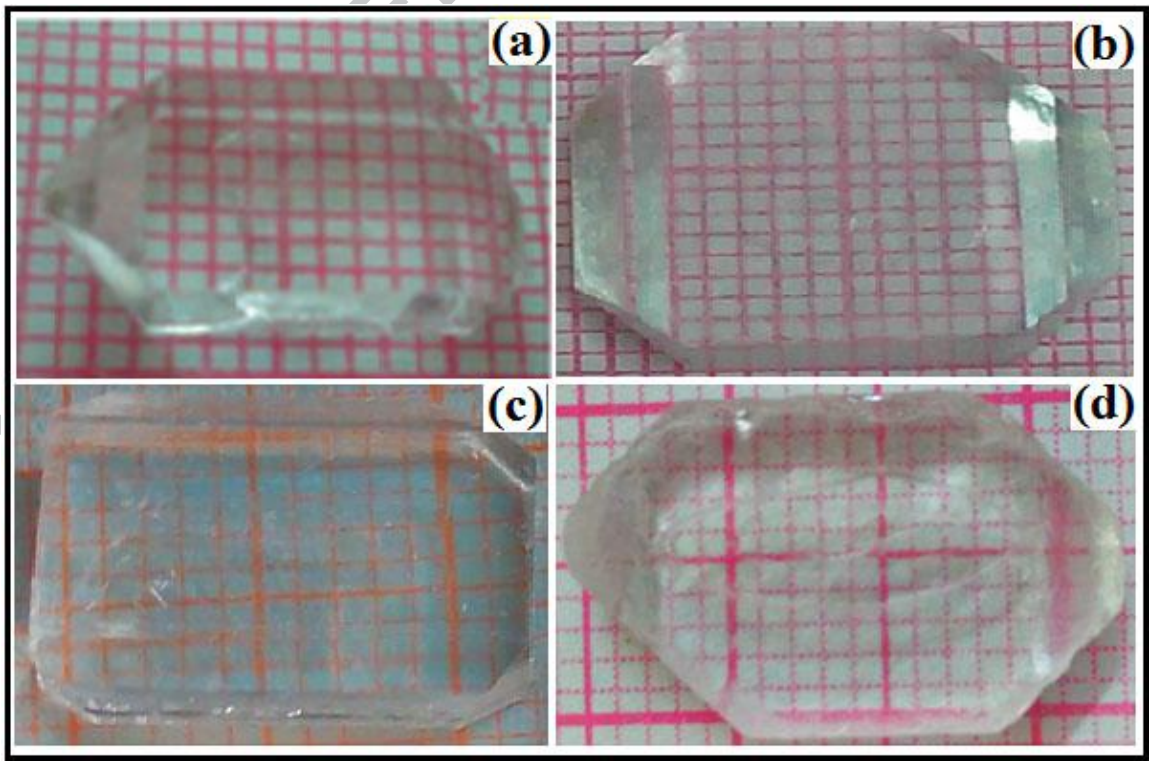


**Fig 1.** Grown crystals of (a) pure (b) 0.4 wt% (c) 0.6 wt% (d) 0.8 wt% L-threonine doped ADP

The qualitative presence of L-threonine in ADP is confirmed by performing paper chromatography. The grown crystals of L-threonine doped ADP is dissolve in distilled water and then the drop of solution is put on filter paper. The one drop of Ninhydrin is dropped on drop of L-threonine doped ADP solution, the area of drop dispersion is marked in circular manner. The droplet mixer spread on filter paper then heated using blow pump and after sometimes the droplet shows characteristic purple spot, which confirms the presence of amino acid (L-threonine) in ADP. The above mention process is schematically described in Figure 2. The same results were obtained for L-threonine doped KDP crystal [9].

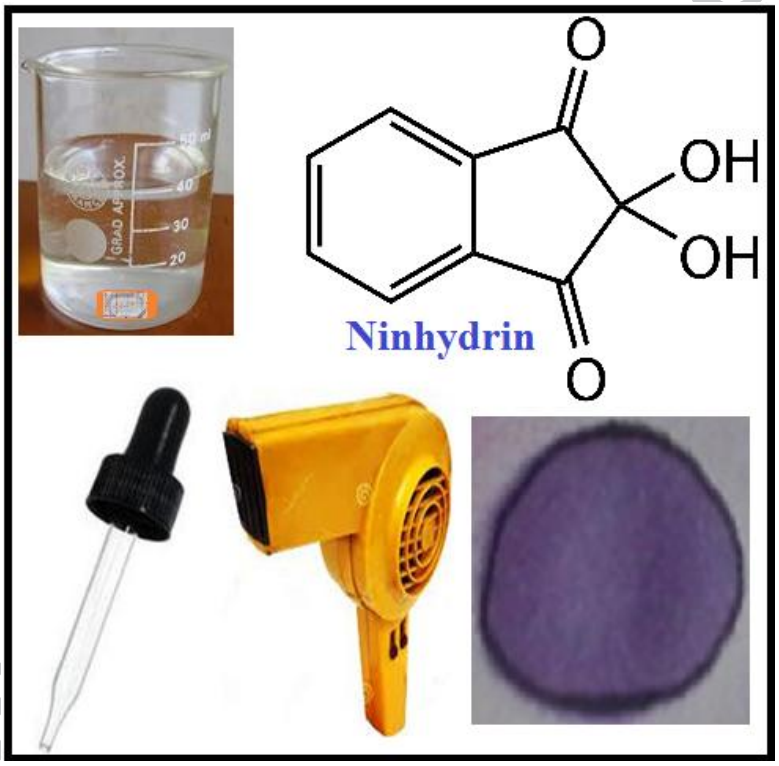


**Fig. 2** paper chromatography of L-threonine doped ADP crystal

The linear refractive index of pure and L-threonine doped ADP crystal is measured by employing prism coupling technique. Initially, the refractive index of organic liquids like toluene and benzene is measured for pre calibration proposes of Abbe's refractometer. Presently, the sodium D line of wavelength 589.3 nm is used. The transparent and surface inclusion free (2 0 0) plane of crystals of pure and L-threonine doped ADP is choose for such study. The grown crystals is placed between the two prisms in which one prism acts as measuring prism and another prism works as illuminating prism. After that, a few drops of methylene iodide is dropped on both prisms and the crystal to make close contact between them. Now the sodium light is incident on the crystal through illuminating prism, which reflects the light on the bottom surface of the reflector prism. The

entire assembly of prisms and crystal is examining by telescope and the difference between the dark and light lines are recorded.

**Characterization Techniques:** The Powder XRD is carried on PHILIPS X'PERT MPD system and the data is analyzed by using powder-X software. The FTIR spectra are recorded in the region 400 – 4000 $cm^{-1}$ using THERMO NICOLET 6700 in KBr media..The FT-Raman spectra are recorded using Bruker RFS 27 spectrometer contains the Nd:YAG laser of power 100 mW, wavelength 1064 nm, scan range of 40 - 4000 $cm^{-1}$ and resolution of 2 $cm^{-1}$. The photoluminescence emission and absoption spectra are recorded at room temperature using Shimadzu RF-5301 PC spectrofluorophotometer and the Xenon is used as exitation source. The CHN analysis is done using Eleementar Vario EL- III in detection range of 0.004 - 30 mg abs for carbon, 0.002-3 mg abs for hydrogen and 0.001-10 mg abs for nitrogen, respectively, where abs stands for absolute range of element detection. The UV-Visible transmittance spectra of single crystals are recorded using Shimadzu UV - 2450 spectrophotometer in the wavelength of 200 - 900 nm. The complex admittance spectroscopy is done for pelletized sample using HIOKI 3532 LCR HITERSTER meter in the frequency range of 100 Hz to 10 MHz and in the temperature range of 323 - 373K. The photoconductivity of polished crystals are carried out using Keithley 485 picometer with the field variation of 5 to 100 V/cm. The SHG efficiency of powdered samples is measured using Q-switched Nd:YAG laser of wavelength 1064 nm and input energy 0.71 J. The Z-scan and Laser thresold damage study of polished and transperent single crystals is done using Abbey refractometer model ATAGO-4T in range of 1.47-1.87, using CW He-Ne laser of wavelength 632 nm, using Nd:YAG laser of Litron Lasers, UK with specification of 1064 nm wavelength, 10 ns pulse width and 35 cm focal length, respectively.

## Results and Discussion:

### 1. Powder XRD

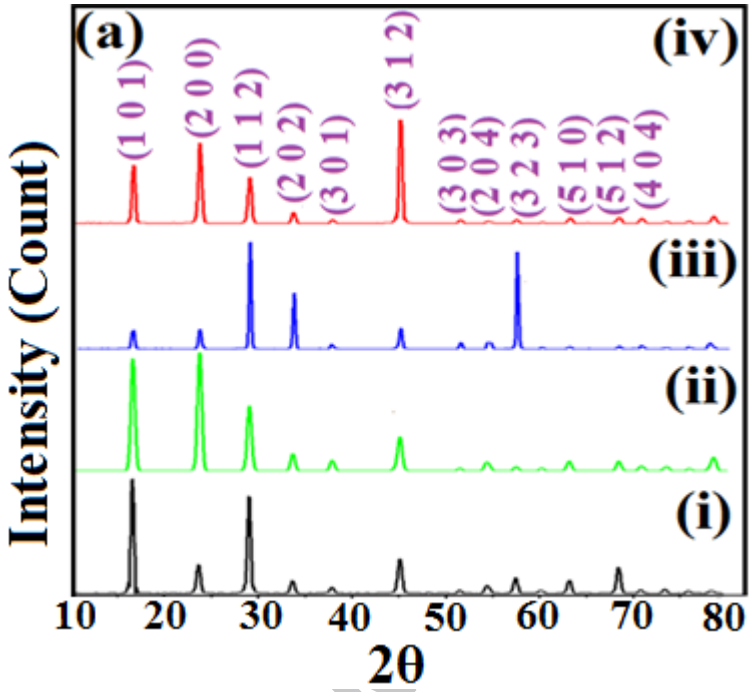


**Fig. 3(a)** Powder XRD spectra of pure and L-threonine doped ADP crystals

The Figure 3 (a) shows the powder XRD patterns of pure and 0.4 wt%, 0.6 wt% and 0.8 wt% L-threonine doped ADP crystals. From the Figure it can be seen that due to doping no additional phase is found to be present and all the crystals possess the single phase nature with characteristic diffraction peaks of ADP, the same result is obtained previous in case of other amino acid doped ADP [10]. The unit cell parameters of ADP crystal match well with standard JCPDS card No. 01-078-2414. The change in diffraction peaks intensity indicating the presence of dopant in ADP. All the crystals are belonged to body centred tetragonal structure symmetry with slight difference in unit cell parameters. The unit cell parameters are listed in table 1.

The minute amount o doping of large size molecule of L-threonine causes the strain in crystalline lattice and that is reflected by the slight change in the unit cell parameters.

| Samples | a = b (Å) | c (Å) | Unit cell volume (Å$^3$) |
|---|---|---|---|
| | ± 0.002 Å | | |
| Pure ADP | 7.505 | 7.550 | 425.25 |
| ADP + 0.4 wt% L-threonine | 7.501 | 7.559 | 425.31 |
| ADP + 0.6 wt% L-threonine | 7.486 | 7.551 | 423.16 |
| ADP + 0.8 wt% L-threonine | 7.499 | 7.540 | 424.01 |

**Table 1.** Unit cell parameters of pure and L-threonine doped ADP crystals

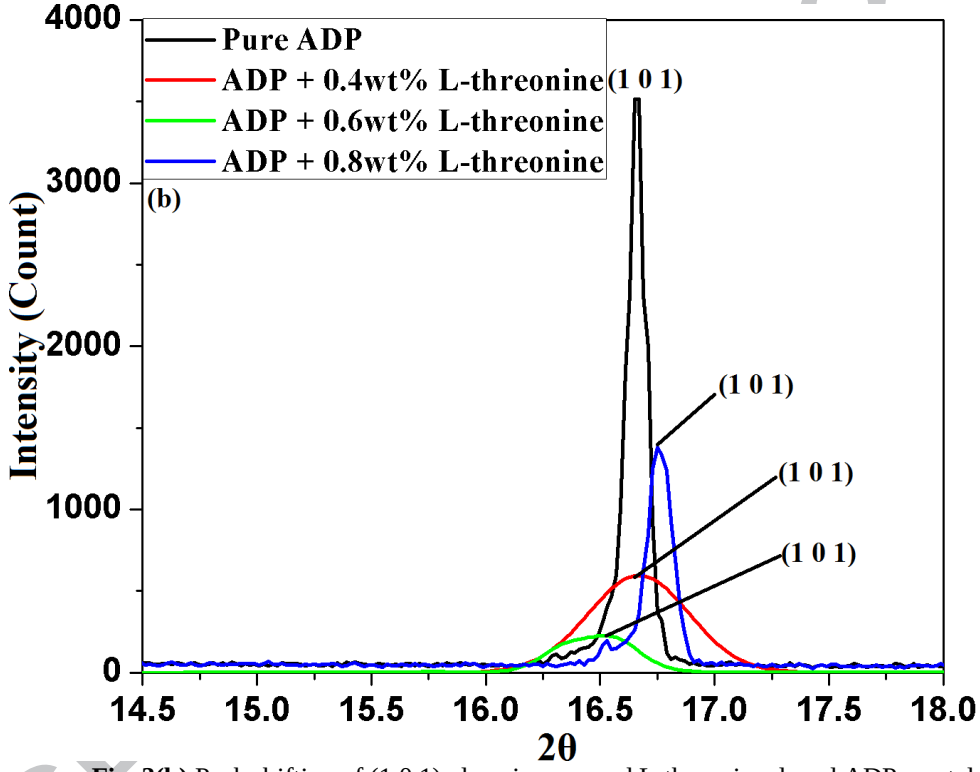


**Fig. 3(b)** Peak shifting of (1 0 1) plane in pure and L-threonine doped ADP crystals

Usually, the amino acid molecule is adsorbed on (1 0 1) plane of ADP [11] and hence the analysis of shifting in (1 0 1) diffraction peak is carried out minutely and shown with expanded scale in Figure 3 (b). Here it is observed that the peak is shifting slightly on doping L-threonine in ADP, also the FWHM increases on doping which is the result of the defect in ADP and strain generated. However, the absence of any additional phase confirms that ADP retains the single phase nature on doping; the only change observed here is that the amino acid molecule causes the lattice distortion upto certain minor extend rather than disturbing the entire lattice structure of ADP.

## 2. FT-IR Spectroscopy

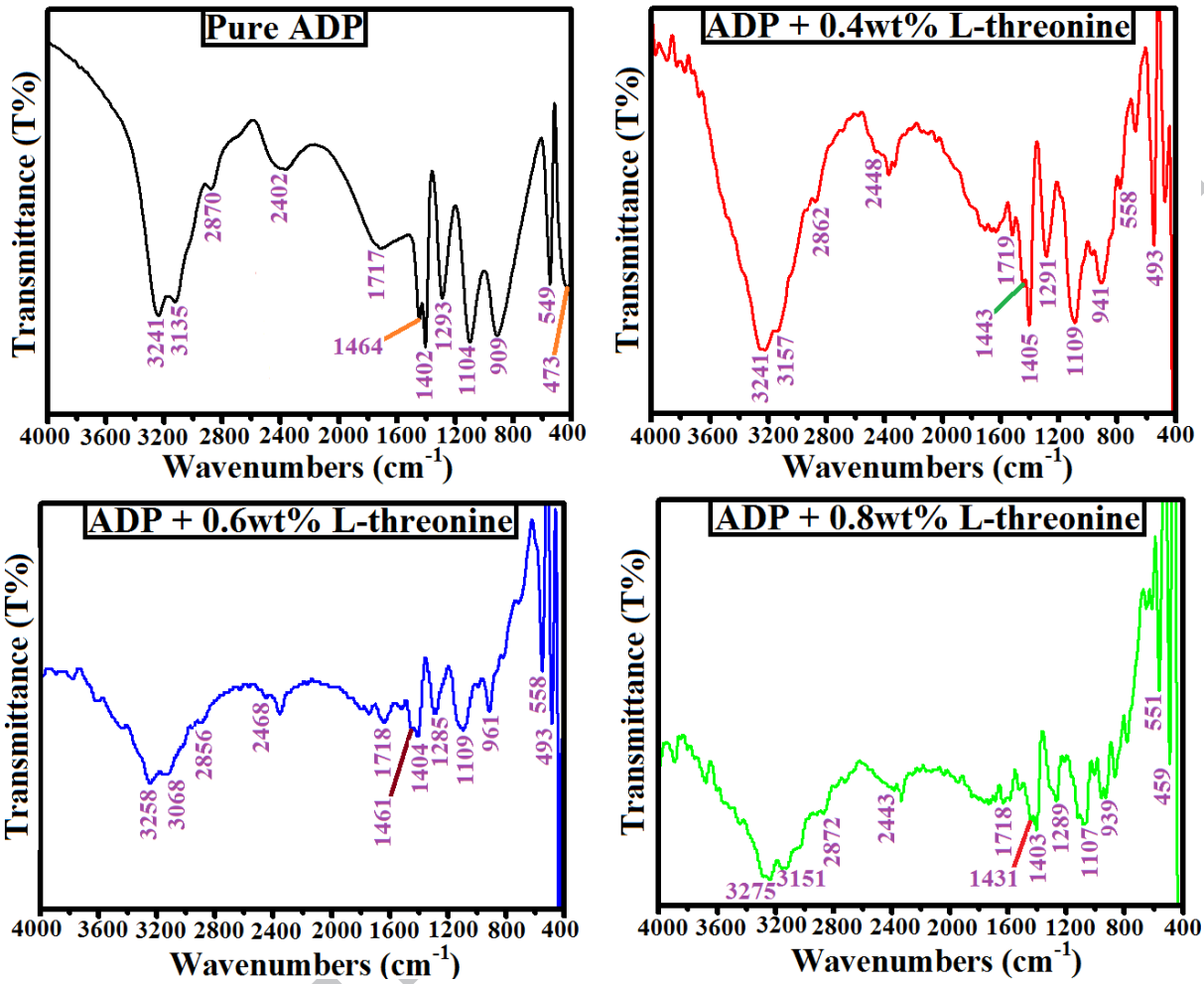


**Fig 4.** FT-IR spectra of pure and L-threonine doped ADP crystals

The influence of amino acid L-threonine with different functional group on ADP is determined by FT-IR spectroscopy. Figure 4 shows FT-IR spectra of pure and L-threonine doped ADP crystals. The L-threonine has shift all the absorption band of ADP as mentioned in table 2. The symmetric stretching of constituent functional group of L-threonine like symmetric stretching of C-H and C=O stretching of COOH group was found in spectra of L-threonine doped ADP crystals. The same results are obtained for L-tartaric acid doped ADP crystal [12].

| Wavenumbers ($cm^{-1}$) | | | | Band Assignment |
|---|---|---|---|---|
| **Pure ADP** | **ADP + 0.4wt% L-threonine** | **ADP + 0.6wt% L-threonine** | **ADP + 0.8wt% L-threonine** | |
| 3241, 3135 | 3241, 3157 | 3258, 3068 | 3275, 3151 | O-H vibration of P-O-H group |
| 2870 | 2862 | 2856 | 2872 | N-H stretching of $NH_4$ and Symmetric stretching of C-H of L-threonine doped ADP |
| 2402 | 2448 | 2468 | 2443 | Hydrogen Bond |
| 1717 | 1719 | 1718 | 1718 | O-H bending, C=O stretching of COOH |
| 1464 | 1443 | 1461 | 1431 | N-H vibration, C-O stretching |
| 1402 | 1405 | 1404 | 1403 | Bending vibration of ammonia |
| 1293 | 1291 | 1285 | 1289 | Combination of asymmetric stretching of $PO_4$ with lattice |
| 1104 | 1109 | 1068 | 1107 | P-O-H stretching, C-O stretching |
| 909 | 941 | 934 | 939 | P-O-H stretching, C-H stretching |
| 549<br>473 | 558<br>493 | 542<br>453 | 551<br>459 | $PO_4$ vibration |

**Table 2.** FT-IR band assignment of pure and L-threonine doped ADP

From the FT-IR band assignments for different functional groups, one can calculate the force constant of diatomic vibrations presents in the sample using standard formulation applying the Hooke's law to the nuclei as a point masses and inter atomic bonds as a mass less spring [13-14].

The doping of L-threonine in ADP expected to produces the L-defect by mean of unoccupied hydrogen vacancy with hydrogen atom of ADP and hence consequently the fundamental vibration of hydrogen is altered. Therefore, the force constant was calculated for O-H vibration, presently.

The relation between the absorption frequency and the force constant can be written as,

$$\upsilon = 1330 \sqrt{F\left(\frac{1}{M_1} + \frac{1}{M_2}\right)} \quad (1)$$

*Where, $\upsilon$ = Absorption frequency ($cm^{-1}$), 1330 = $(N_A \times 10)^{1/2} / 2\pi C$, $N_A$ = Avogadro's number, F = Force constant ($Nm^{-1}$), $M_1$ and $M_2$ = Molecular masses of atoms (u).*

From the table 3 it can be seen that the force constant gets altered as the amino acids interacts with the hydrogen bond of ADP.

| Sample | Force constant of O-H Vibration ($N.m^{-1}$) | Absorption Wavenumber ($cm^{-1}$) |
|---|---|---|
| Pure ADP | 526 | 3135 |
| ADP + 0.4wt% L-threonine | 534 | 3156 |
| ADP + 0.6wt% L-threonine | 504 | 3068 |
| ADP + 0.8wt% L-threonine | 532 | 3151 |

**Table 3.** Force constant of O-H vibration for pure and L-threonine doped ADP crystal

## 3. FT-Raman spectroscopy

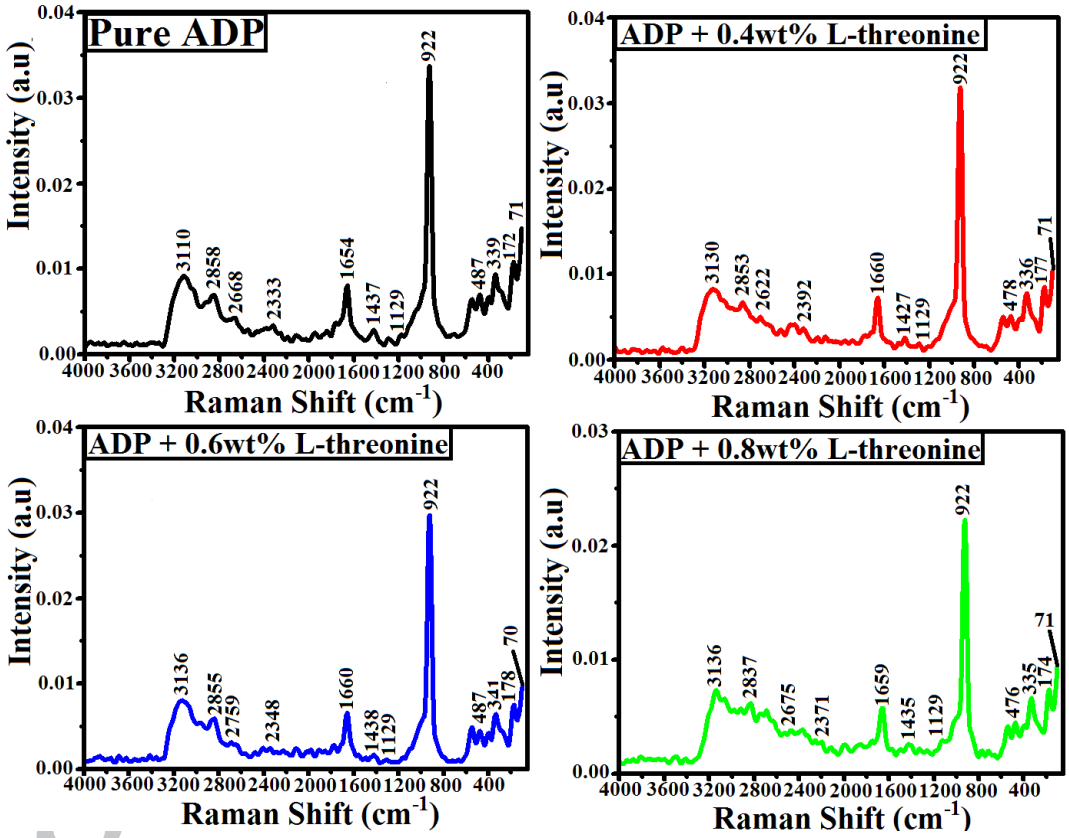


**Fig 5.** FT-Raman spectra of pure and L-threonine doped ADP crystals

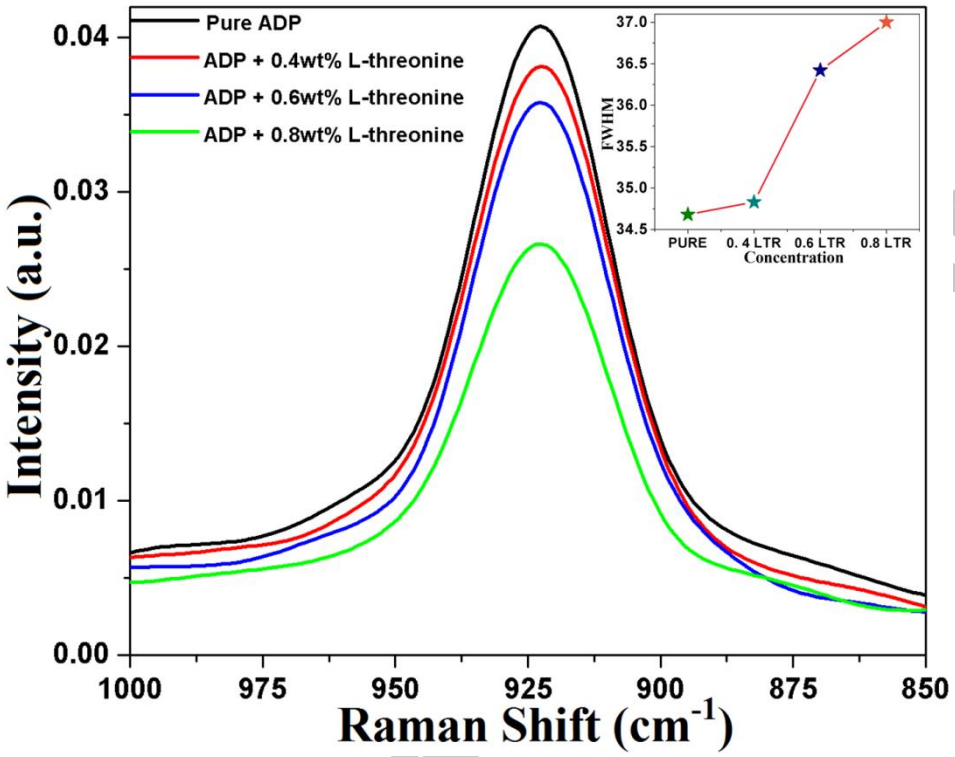


**Fig. 6** Intensity variation of [$PO_4$] group in pure and L-threonine doped ADP crystals

The Figure 5 shows the FT-Raman spectra of pure and L-threonine doped ADP. The spectra exhibit all the normal modes of vibrations for $NH_4^+$ and $PO_4^{3-}$ groups of ADP. The band assignment corresponds to the various normal modes of vibration is listed in table 4. The obtained data are compared with the standard data available in the literature for pure ADP [15-16].

| Pure ADP | ADP + 0.4 wt% L-threonine | ADP + 0.6 wt% L-threonine | ADP + 0.8 wt% L-threonine | Band Assignment |
|---|---|---|---|---|
| 3110 s | 3130 s | 3136 s | 3136 s | $\nu_1$ ($NH_4$) |
| 2858 sh | 2853 sh | 2855 sh | 2837 sh | ν O-H |
| 2668 sh | 2622 sh | 2759 sh | 2675 sh | ν O-H |
| 2333 sh | 2392 sh | 2348 sh | 2371 sh | ν O-H |
| 1659 m | 1660 m | 1660 m | 1659 m | $\nu_2$ ($NH_4$) |
| 1437 vw | 1427 vw | 1438 vw | 1435 vw | $\nu_4$ ($NH_4$) |
| 1129 w | 1129 w | 1129 w | 1129 w | $\nu_3$ ($PO_4$) |
| 922 s | 922 s | 922 s | 922 s | $\nu_1$ ($PO_4$) |
| 487 m | 478 m | 487 m | 476 m | $\nu_4$ ($PO_4$) |
| 339 m | 336 m | 341 m | 335 m | $\nu_2$ ($PO_4$) |
| 172 m | 177 m | 178 m | 174 m | T ($PO_4$) + R ($PO_4$) |
| 71 s | 71 s | 70 s | 71 s | R ($PO_4$) |

ν = Stretching, T = Translation, R = Rotation, s = strong, sh = shoulder, m = medium, w = weak, vw = very weak

**Table 4.** FT-Raman band assignment of pure and L-threonine doped ADP

Further, the Figure 6 shows the $\nu_1$ group symmetry of $PO_4$ group of pure and L-threonine doped ADP crystals which corresponds to the O-H.....O bond stretching vibration. From the Figure, it can be seen that the peak position i.e. 922 $cm^{-1}$ does not shift on doping suggesting that the framework of $PO_4$ group retains its original position in lattice matrix ADP, but the Figure indicating that by doping the amino acid in ADP the FWHM of peak increases and intensity of peak decreases. This may due to fact that dopant causes the defect in hydrogen bonding (O-H.....O) of ADP and leads to increase the bond distance, hence the bond length and stretching vibration of O-H.....O increases, which decreases the intensity of that peak.

## 4. Photoluminescence (PL) Study

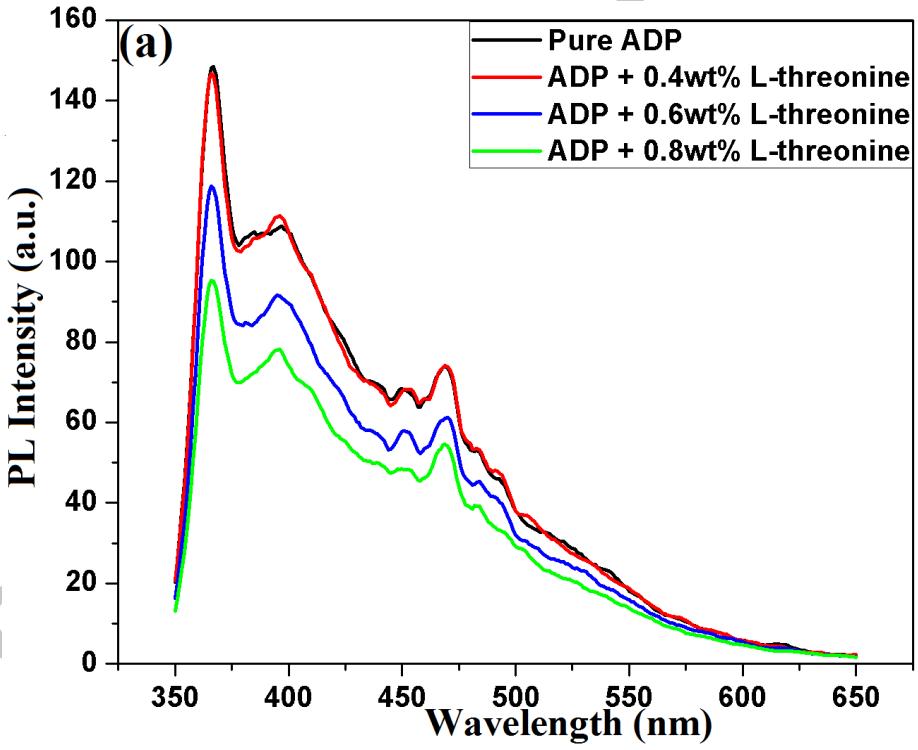


**Fig. 7(a)** PL emission spectra of pure and L-threonine doped ADP

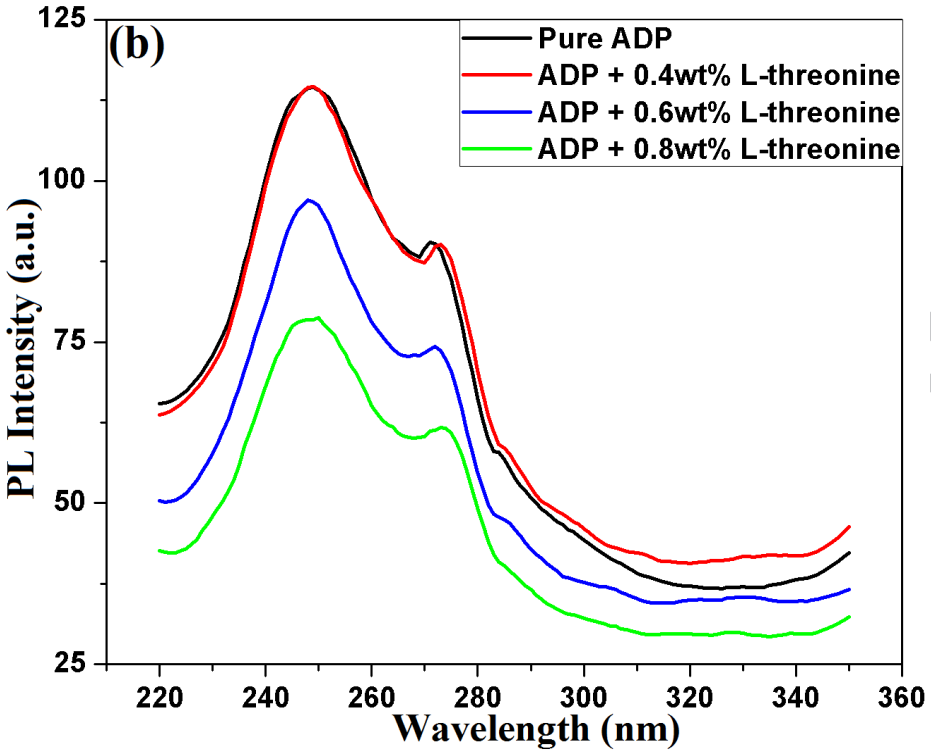


**Fig. 7(b)** PL absorption spectra of pure and L-threonine doped ADP

To investigate the quality of grown crystals, the qualitative measurement of impurity incorporation and the optical phenomena like recombination of the electron transitions, the photoluminescence emission study at particular wavelength becomes a pioneer technique [17].

The Figure 7(a) shows PL emission spectra of pure and L-threonine doped ADP samples. The PL excitation wavelength is 254 nm and emission wavelength is 280 nm.

The spectra exhibits two emission peaks at different wavelength, as listed in table 5.

| Sample | Emission Wavelength | |
|---|---|---|
| Pure ADP | 367.92 nm | 469.94 nm |
| ADP + 0.4wt% L-threonine | 365.90 nm | 468.93 nm |
| ADP + 0.6wt% L-threonine | 366.13 nm | 469.47 nm |
| ADP + 0.8wt% L-threonine | 367.14 nm | 470.48 nm |

**Table 5**. PL emission peaks for pure and L-threonine doped ADP

From the table 5 it can be observed that 0.4 wt% L-threonine doped ADP sample shows the maximum blue shift of emission peaks compared to the pure ADP samples, while the other samples like 0.6 wt% and 0.8 wt% L-threonine doped ADP exhibit progressively less blue shift in the emission compared to the pure ADP sample. Further, it can be seen from the Figure 7(a) that the intensity of PL emission spectra decreases as the concentration of amino acid dopant increases, which suggests the incorporation of dopant (L-threonine) within pure ADP.

The emission peak around 2.6 eV (365-367nm) is due to an electron recombination on the trapped hole centre on the bases of hydrogen vacancy (L-defect or A-radical) and the emission peak around 3.6 eV (468-470nm) is due to recombination of hole at the electron centre on the bases of double occupied hydrogen vacancy (D-defect or B-radical).

The intensity of PL emission spectra can be correlated with the electrical conductivity of material. Usually, the intensity of PL emission spectra is small for the material having larger electrical conductivity. Hence, the PL emission study reveals that the doping of amino acid (L-threonine) causes defect in structure of ADP [18].

The Figure 7(b) shows PL absorption spectra of pure and L-threonine doped ADP. In a given material, for a same electronic transition, the difference of wavelengths between the position of the band maxima of absorption and emission spectra gives rise to Stokes shift [19].The Stokes shift is observed when the energy of emitted photon is less compared to absorbed photon and anti-Stokes shift observed when the energy of emitted photon is more compare to absorbed photon [20].

Presently, the energy difference between emission and absorption band maxima is taken into account for pure and L-threonine doped ADP samples. The table 5 shows Stoke shift variation for pure and doped samples.

| Sample | Energy absorption (eV) | Energy emission (eV) | Stoke shift (eV) |
|---|---|---|---|
| Pure ADP | 4.9877 | 3.4055 | 1.5822 |
| ADP + 0.4wt% L-threonine | 4.9877 | 3.3903 | 1.5974 |
| ADP + 0.6wt% L-threonine | 4.9984 | 3.3903 | 1.6080 |
| ADP + 0.8wt% L-threonine | 5.0068 | 3.3903 | 1.6164 |

**Table 6**. Variation of Stoke shift of pure and L-threonine doped ADP

The Stoke shift in solid material occurs due to the phenomena called vibrational energy (or population) relaxation [21]. In the condensed matter, under the course of electromagnetic radiation, the relaxation of molecules occurs usually by the interaction with environment of lattice. The lattice forms a continuum of intermolecular motion that can annihilate the energy of the vibrational relaxer, which leads to produce the excitation of lattice motion at higher level energy state [22].

The Photoluminescence observed in ADP is due to its crystallographic and electronic structure. At room temperature, its electronic structure may determine mainly by the anionic $H_2PO_4$ group.

The electronic transition in ADP and occurrence of large Stoke shift is explained as follows: The upper occupied molecular orbits of $H_2PO_4$ anionic group, whose energy position corresponds to the valance band of

ADP are formed from almost pure 2Pπ oxygen orbits, while the lowest unoccupied bands are formed of 1S hydrogen orbits. The electronic transition with the lowest energy in the $H_2PO_4$ group is due to the transfer of an electron between the above mentioned energy levels [23].

Further, at low temperature, in ADP, there will be existence of self-trapping of holes with formation of $[H_2P_O4]^0$ radical. This existence is strongly gives the evidence of Self Trapped Excitons (STE). The STE in ADP is a result of recombination of electrons at self-trapped hole. The radiation annihilation of such STE leads to produce large Stoke shift in ADP.

Now, the crystallographic defect point of view in pure and L-threonine doped ADP can be understood in following way: The crystal of pure ADP consists of several type of intrinsic lattice defects, among them the simplest are orientational defects namely the unoccupied hydrogen vacancy (L-defect) and the double hydrogen bond (D-defect). Further, Hasmuddin et al. have listed variety of dopant concentration dependant crystallographic defect crystals [12].

At low temperature, in ADP, the free radical is formed called A radical (L-defect) by a regular anionic group $[H_2PO_4]^-$ , where one proton of the hydrogen bond is lost. This defect form a localized structure called hole at an oxygen ion near a hydrogen vacancy.

For the formation of A-radical in ADP, two mechanism are proposed, the first mechanism exists in crystal is ionized according to the scheme $L + h^+ \rightarrow L^+ = A = [H_2PO_4]^-$ , and the second mechanism is the radiation induced generation of band electrons and holes. In this process, by trapping an electron, the hydrogen ion transforms into a neutral hydrogen atom $H_0$, which is displaced from the lattice site, while the trapping of a hole by an oxygen atom, nearest to the vacancy formed leads to the formation of an A radical [24].

The intensity of PL emission spectra of doped ADP is decreases compare to pure ADP suggesting that when the amino acid molecule is introduced in ADP lattice matrix, the dopant will destabilized the orientational L-defect in the vicinity of impurity atoms for the compensation of the charges.

The electric studies of pure and L-threonine doped ADP supports above mention arguments because it is found that the dopant causes the hydrogen vacancy in ADP lattice and leads to increase the conductivity compare to pure ADP.

From the table 6, it can be observed that on increasing the doping concentration of L-threonine, the Stoke shift is increase. Such behaviour can be understood by following way: The dopant L-threonine have positive $NH_3^+$ and negative $COO^-$ charge, that forms a dipole which is surrounded by ADP lattice. When L-threonine enters into the excited state under the influence of electromagnetic radiation, its dipole moment will change, but the ADP lattice is not able to adjust with this change so quickly. Hence when the vibration relaxation occurs in system the dipole moments of them will get realign with respect to applied optical field. Therefore, on increasing the doping concentration of L-threonine, it will become quite difficult for ADP lattice to realign and as a result there will be increment of Stoke shift in ascending order of doping.

## 5. CHN Analysis

The CHN analysis of L-threonine doped ADP samples is listed in table 6. From that table, one can notice that on increasing doping concentration of amino acid L-threonine in ADP, the percentage of carbon, hydrogen and nitrogen increases which confirms the successful doping of L-threonine in ADP.

| Sample | C % | H % | N % |
|---|---|---|---|
| Pure ADP | - | 5.23 | 12.00 |
| ADP + 0.4wt% L-threonine | 0.07 | 5.45 | 12.02 |
| ADP + 0.6wt% L-threonine | 0.09 | 5.50 | 12.06 |
| ADP + 0.8wt% L-threonine | 0.10 | 5.56 | 12.14 |

**Table 7.** CHN analysis data of L-threonine doped ADP

Although, on increasing doping concentration of L-threonine in ADP the amount of carbon is increases but the concentration of carbon is not obtained exactly than the concentration of L-threonine is added at the time of crystal preparation. This difference can be understood on the basis of solubility difference. The solubility of ADP and L-threonine at room temperature is 46 gram / 100 millilitre and 10.6 gram / 100 millilitre, respectively. Therefore, during course of crystal growth it is expected that the ADP solidifies faster than L-threonine and as a result there will be limited amount of dopant enters into lattice sites of ADP as per the expectation. Besides this, the XRD study revel that upon doping the L-threonine in ADP, the ADP retains the single phase nature and the L-threonine also consist of atoms like nitrogen and hydrogen same as of ADP hence the segregation of dopant and host may not possible presently

## 6. UV-Visible Spectroscopy

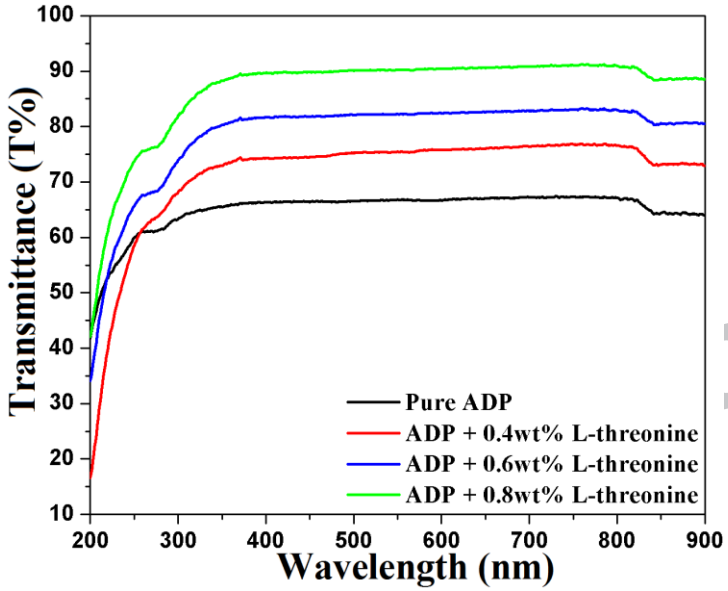


**Fig 8.** Transmittance spectra of pure and L-threonine doped ADP crystals

The Figure 8 shows optical transmittance spectra of pure and L-threonine doped ADP crystals. The thickness of grown crystals are 6.07 mm, 3.22 mm,4.12 mm and 1.56 mm for pure, 0.4 wt%, 0.6 wt% and 0.8 wt% L-threonine doped ADP crystals, respectively. The spectra exhibit high transparancy in the entire visible region. The optical transmittance increases uniformly with doping concentration of L-threonine in ADP. The maximum transmittance for pure, 0.4 wt%, 0.6 wt%, and 0.8 wt% L-throenine doped ADP crystals is found to be 67.43%, 76.92%, 83.27% and 91.27%, respectively.

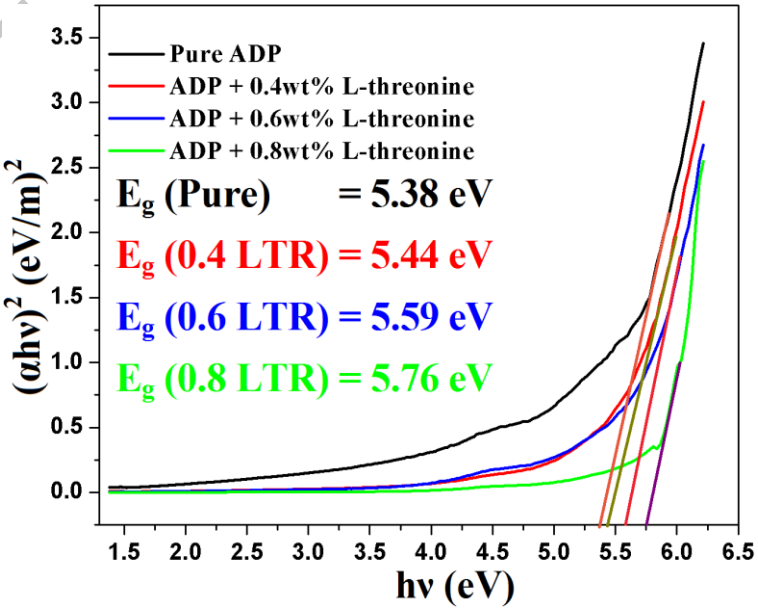


**Fig 9.** Tauc's plots of pure and L-threonine doped ADP crystals

The absorption coefficient (α) is calculated from the transmittance data using the following experssion,

$$\alpha = \frac{2.303\ log_{10}(\frac{1}{T})}{d} \quad (2)$$

*Where, T = Transmittance, d = Thickness of crystal.*

The optical energy band gap($E_g$) was determined from the transmittance and optical absorption coeffcient (α) near the absorption edge using the equation,

$$\alpha hv = A(hv - Eg)^2 \quad (3)$$

*Where, h = Planck's constant, v = Frequency, $E_g$ = Optical band gap and A = Constant.*

The optical energy band gap ($E_g$) of pure and L-threonine doped ADP crystals are determined from Tauc's plot by extrapolating straight line on X-axis, as shown in the Figure 6. The optical energy band gap of pure and 0.4 wt%,0.6 wt% and 0.8 wt% L-threonine doped ADP crystal is found 5.38 eV, 5.44 eV, 5.59 eV and 5.76 eV, respectively. The high values of energy band gaps of pure and doped ADP crystals makes them suitable for fabrication of optoelectronic devices [25].

For the Nonlinear optical applications, the large band gap crystal is needed because the energy band gap of crystal shows the ability of dielctric medium (crystal) to be polarized under the influence of powerful radiation. Here the obtained $E_g$ values for pure and L-threonine doped ADP crystals are found to be quite superior than the other amino acids doped ADP crystals like L-alalnine, L-valaine, L-cystine, L-lysine and L-glycine etc. [26-30].

The refractive index of pure and L-threonine doped ADP crystals are calculated using the following expression [31],

$$n = \frac{1}{T} + \left(\frac{1}{T} - 1\right)^{1/2} \quad (4)$$

*Where, n = refractive index, T = transmittance.*

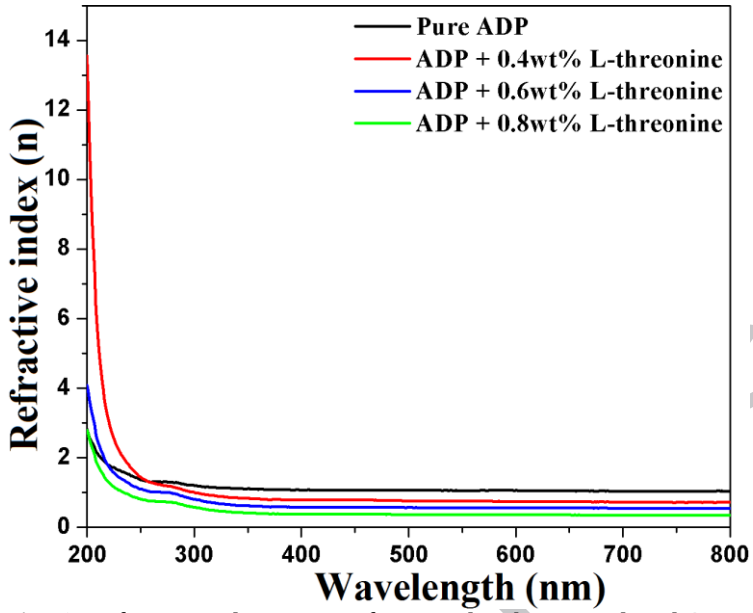


**Fig 10.** Refractive index spectra of pure and L-threonine doped ADP crystals

The Figure 10 shows the variation of refractive index with respect to wavelength for pure and L-threonine doped ADP crystals. The refractive index for all the samples decreases as wavelength increases.Alike the behaviour of the optical transmittance, the magnitude of refractive index for doped samples decreases progressively on increasing the doping and it is quite lower compared to the pure one. The high transmittance and lower refractive index of doped samples makes them promissing candidates for antireflection applications [32].

As ADP being a NLO material and belongs to tetragonal crystal system, here the ordinary and extra ordinary refraractive indices are calculated using the following expression:

$$n_0 = 2.302842 + \frac{0.01125165}{\lambda^2 - 0.013253659} + \frac{15.102464\lambda^2}{\lambda^2 - 400} \quad (5)$$

$$n_e = 2.163510 + \frac{0.009616676}{\lambda^2 - 0.01298912} + \frac{5.919896\lambda^2}{\lambda^2 - 400} \quad (6)$$

*Where, $n_0$ = Ordinary – ray refraractive index, $n_e$ = Extra ordinary – ray refractive index, $\lambda$ = Wavelength.*

The obtained values of $n_0$ and $n_e$ for ADP is 1.45 and 1.42, respectively. Hence $n_0 > n_e$ corrosponds to negative unixial nature of ADP crystal and it can be use for birefriengence applications.

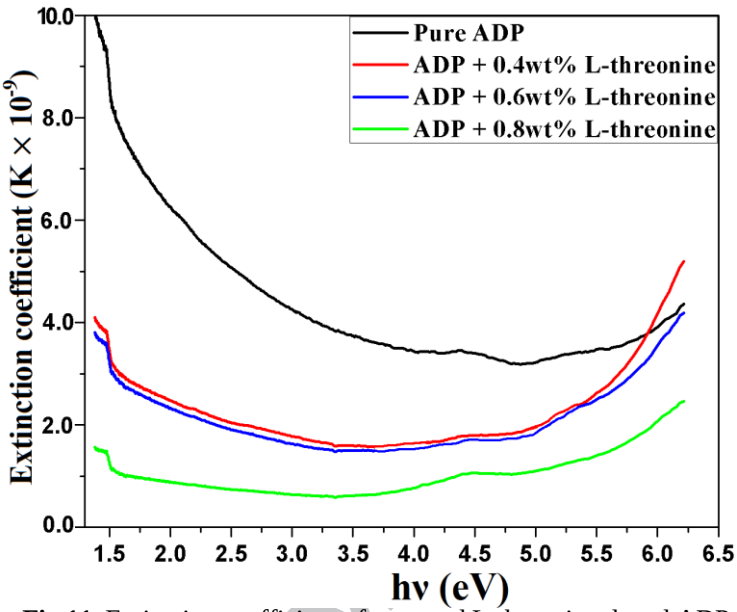


**Fig 11.** Extinction coefficient of pure and L-threonine doped ADP crystals

The extinction coefficient is a measure of the fraction of light lost due to scattering and absorption per unit distance of the participating medium.

The extinction coefficient (K) of grown crystals is numerated using following relation,

$$K = \frac{\lambda \alpha}{4\pi} \tag{7}$$

*Where, λ = Wavelength, α = Absorption coefficient.*

The Figure 11 shows the variation of extinction coefficient as a function of photon energy (hν) for pure and L-threonine doped ADP crystals. The extinction coefficient of all crystals decreases as the photon energy increases suggesting that the fractional loss of incident radiation on crystal decreases and at higher photon energy it is slightly increases this may be due to scattering and absorption behaviours depending on photon energy and nature of scattering centres.

The magnitude of extinction coefficient is quite lower and uniform for L-threonine doped ADP compared to the pure ADP. This result is in harmony with refractive index and transmittance results.

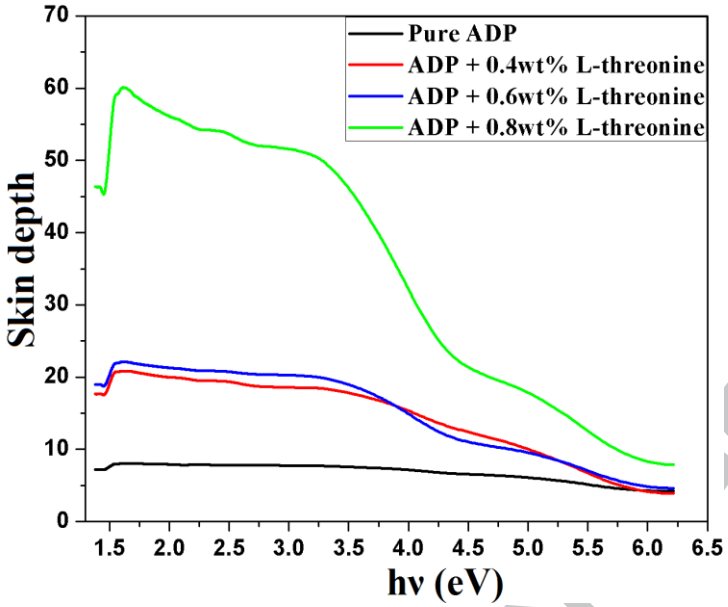


**Fig 12.** Skin depth of pure and L-threonine doped ADP crystals

The skin depth (δ) is defined as amount of penetration of electromagnetic radiation into a material. Numerically, it is define as,

$$\delta = 1 / \alpha \qquad (8)$$

*Where, δ = Skin depth, α = Absorption coefficient.*

The Figure 12 shows the variation of skin depth with respect to photon energy for pure and L-threonine doped ADP crystals. The skin depth increases slightly in the lower photo energy region with small peaks and then it is decreases as the photon energy increases for all crystals, however, this behaviour becomes more prominent as the doping increases. Also, the peak shifting toward the higher photon energy region occurs as the doping concentration of L-threonine increases in ADP crystal. The magnitude of skin depth increases with increase in doping concentration of L-threonine in ADP crystal. This result indicates that the skin depth of grown crystals is directly related to transmittance of crystals [33].

Hence, the entire course of optical study suggests that the L-threonine doped ADP crystals with higher transmittance, skin depth, enhanced energy band gap, lower refractive index and extinction coefficient find the variety of applications in optoelectronics.

## 6.1 Wemple-DiDomenico single oscillator model analysis

Wemple and DiDomenico [34] have devloped a single oscillator model for the inter band transition of electrons in brillouin zone, which behaves as an individual oscillator and recognizes that the valence electrons of atoms contribute to one such oscillator. For the nonlinear optical applications this model is useful to study the dependence of refractive index below the band gap energy region (inter band absorption edge).

The dependence of refractive index on photon energy below inter band absorption edge ($h\nu < E_g$) is given as,

$$n^2(\lambda) = 1 + \frac{E_o E_d}{({E_0}^2 - E^2)} \quad (9)$$

*Where , $E_0$ = Single oscillator energy, $E_d$ = Dispersion energy, $E = h\nu$ = Photon energy*

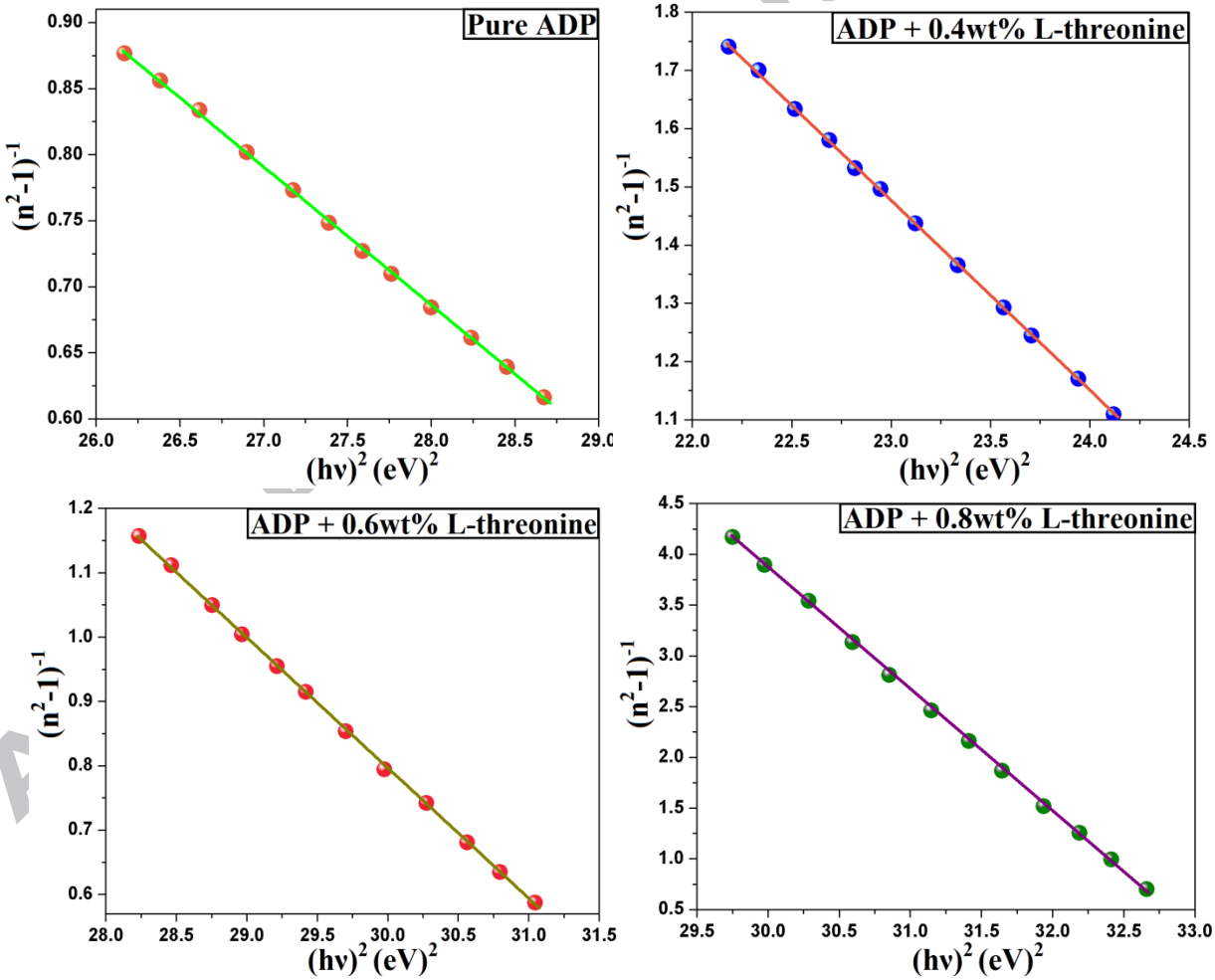


**Fig. 13(a-d)** Wemple-DiDomenico model plots for pure and L-threonine doped ADP crystal

The Figure 13 (a-d) shows the dispersion of refractive index with respect to photon energy below the absorption edges of pure and L-threonine doped ADP. The linear fitting of above mentioned plot gives intercept and slope. The dispersion parameters like $E_0$ and $E_d$ is calculated using below mentioned expressions.

$$E_d = \sqrt{\frac{1}{Intercept \times Slope}} \qquad E_0 = E_d \times Intercept \tag{10}$$

The parameter $E_0$ corresponds to the distance between centers of gravity of the valance and conduction band, while the other parameter $E_d$ corresponds to the average strength of the inter-band optical transitions.

Further, the values of moments of single oscillator dispersion spectra are calculated according to the following experssion [35],

$$M_{-1} = \frac{E_d}{E_0}, \quad M_{-3} = \frac{E_d}{E_0^3} \tag{11}$$

| Sample | $E_d$ (eV) | $E_0$ (eV) | $M_{-1}$ | $M_{-3}$ |
|---|---|---|---|---|
| Pure ADP | 1.63 | 5.58 | 0.27681 | 0.00801 |
| ADP + 0.4wt% L-threonine | 0.58 | 5.25 | 0.11144 | 0.00405 |
| ADP + 0.6wt% L-threonine | 0.85 | 5.83 | 0.14544 | 0.00429 |
| ADP + 0.8wt% L-threonine | 0.14 | 5.76 | 0.02514 | 0.00076 |

**Table 8.** Dispersive parameters of pure and L-threonine doped ADP crystals

From the table 8 it can be seen that the dispersive parametes decreases for L-threonine doped ADP crystals compared to the pure one. This can be interpreted as follows.The single oscillator energy ($E_0$) is related to the avergage bond strength of material known as the cohesive energy. The cohesive energy defined as the difference between the average energy of the free atoms and that of the atoms of a crystal.

Further, as per the chemical bond approch [36], atoms combine more favorably with atoms of diffrent kind rather that with the same kind and during the course of combination the bonds will be formed which ultimetly decreases the bond energies untill all the available valences are satisfied.

Therefore, in the present system the incorporation of L-threonine in ADP is sucessfully expected, which combines with the ADP lattice materix by mean of lowering the bond energy and ultimetly reduces the single oscillator energy as per the above mentioned model.

Moreover, one can see from the above table that the 0.4wt% L-threonine doped ADP crystals have possese least single oscillator energy among the other concentation which favors the incorporation of threonine at greater extend and hence crystal with this concentration may have superior nonlinear optical properties as explained in following section.

## 7. Complex Admittance spectroscopy

The complex admittance (*Y**), defined as reciprocal of complex impedance (*Z**), is able to measure the capacitance (C) and conductance (G) of material. It is able to indicate surface region phenomena like formation of the interfacial layer and impurity concentration within a sample [37].

To obtain capacitance (*C*) and conductance (*G*) of pure and L-threonine doped ADP, the following relation between complex permittivity (ε*) and complex admittance (Y*) was taken into account [38],

$$Y^* = Y' + iY'' = G + i\,C \tag{12}$$

$$\varepsilon^* = \frac{Y^*}{i\omega C_0} = \frac{C}{C_0} - i\,\frac{G}{\omega C_0} \tag{13}$$

*Where, C = Capacitance, G = Conductance, $C_0$ = Vacuum capacitance = $\varepsilon_0 A / d$, $\varepsilon_0$ = Permittivity of free space, A = Cross section area of pellet and d = Thickness of pellet.*

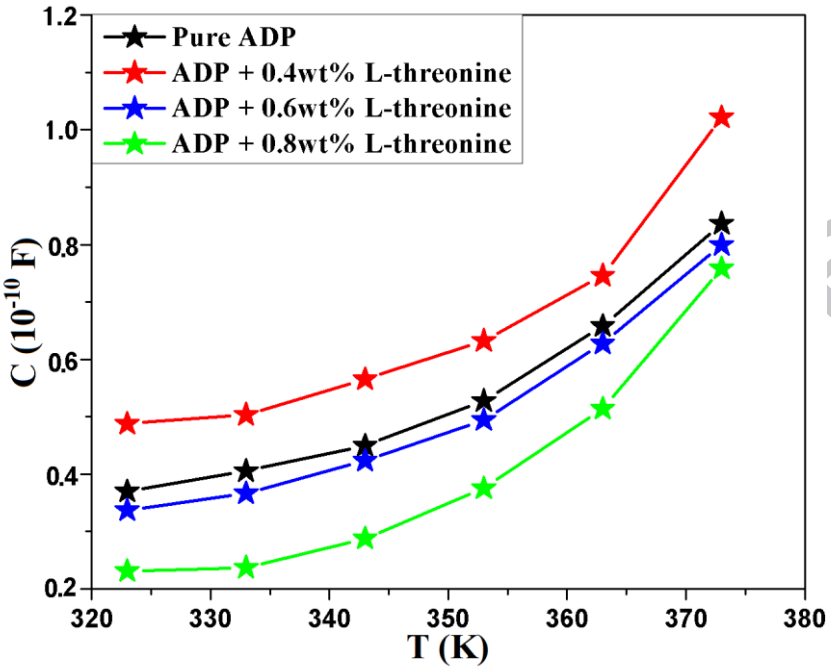


**Fig.14** capacitance versus temperature of pure and L-threonine doped ADP at $\omega = 100$ rad.s$^{-1}$

The Figure 14 shows variation of capacitance with respect to temperature at an angular frequency 100 rad.s$^{-1}$ for pure and L-threonine doped ADP. The capacitance is a function of dielectric constant suggesting amount of polarization of dipoles under the influence of a.c.electric field.

The capacitance of all samples increases as the temperature increases, which may due to the increase of thermally activated charge carrier mobility and formation of interfacial space charge formation at electrode-electrolyte interface [37].

Further, by comparing the magnitude of capacitance it is observed that the 0.4wt% L-threonine doped ADP have higher capacitance among the other samples.

The fact considered here is that the capacitance of material is directly proportional to the dielectric constant and as per the Clausius-Mosotti relation [39] correlating the polarizibility with second harmonic generation efficiency of NLO material theoretically; the dielectric constant is directly proportional to polarizibility. Therefore, it is interesting to verify experimentally that the 0.4wt% L-threonine doped ADP with highest capacitance may have highest dielectric constant and polarizibility among the other doping concentration of L-threonine in ADP. Ultimately, the material with highest polarizibility may have highest second harmonic generation (SHG) efficiency and as the induced polarization of nonlinear medium by laser is directly proportional to the second order, third order nonlinear optical susceptibility, the relation holds true

presently. The second and third harmonic generation efficiency of all grown crystals is discussed in forthcoming section.

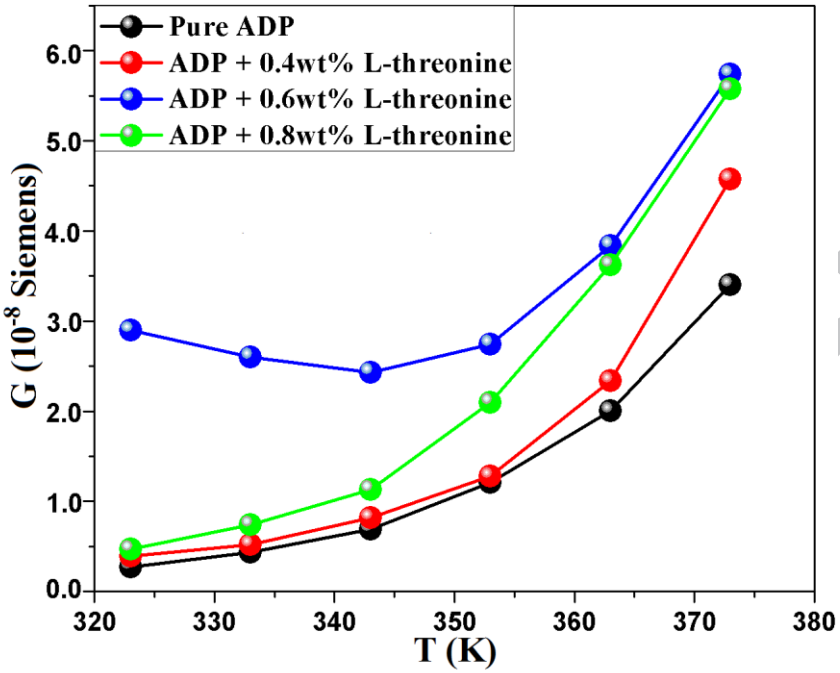


**Fig.15** Conductance versus temperature of pure and L-threonine doped ADP at ω = 100 rad.s$^{-1}$

The Figure 15 shows the variation of conductance with respect to temperature at an angular frequency 100 rad.s$^{-1}$. The conductance is function of charge carrier motion i.e. proton motion in the structure of single crystal. The conductance of all samples increases with increase in temperature suggesting thermally activated process present within the samples. The magnitude of conductance is more for L-threonine doped ADP samples compared to the pure ADP suggesting that the conductivity increases for L-threonine doped ADP samples compared to the pure one. The 0.6 wt% L-threonine doped ADP has the highest magnitude of conductance among the other doping concentration of L-threonine in ADP. For the 0.6wt% L-threonine doped ADP the reason behind highest conductance is that, the 0.6 wt% concentration of dopant (L-threonine) causes highest defect called hydrogen vacancies in ADP and hence as the conduction in ADP is protonic, that will leads to produced highest magnitude of conductance.

As the ADP being hydrogen bonded crystal, hydrogen bond is responsible for the electrical conductivity in ADP crystal. By doping the amino acid in ADP crystal, the dopant molecule causes the defect in lattice matrix of ADP in two ways, namely, the hydrogen vacancy (L-defect) and the doubled occupied bond (D-defect), which are responsible for electrical conduction in ADP crystal [40]. The L and D defects in ADP unit cell is illustrated in Figure 17.

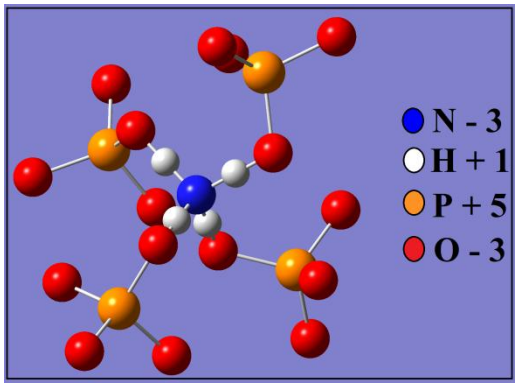


**Fig 16.** ADP unit cell

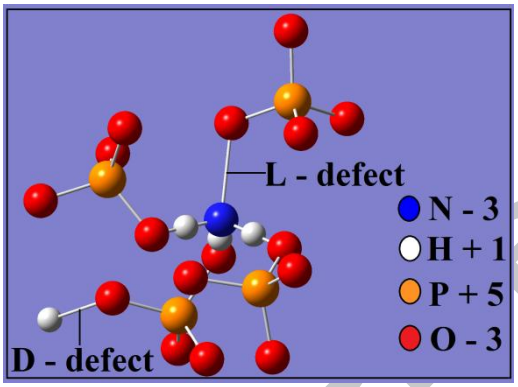


**Fig.17** Defects in ADP unit cell

Moreover, the conductance curves for pure, 0.4wt% and 0.8wt% L-threonine doped ADP samples show a single slope suggesting one conduction mechanism throughout the temperature range considered, while the same for 0.6 wt% L-threonine doped ADP shows that the slope of curve changes at two different temperature regimes suggesting two different conduction mechanism present within a sample.

The different conductance mechanism of all samples over temperature range considered is determined by Jonscher's power law [41] to the conductivity of pure and doped ADP, and found that for pure, 0.4wt%, 0.6wt% (353-373K) and 0.8wt% L-threonine doped ADP crystal the Correlation barrier hopping (CBH) mechanism is exist while that of for 0.6wt% L-threonine doped ADP (323-343K) temperature range the Nonoverllaping small polaron tunnelling (NSPT) conduction mechanism is prevailing, hence the conduction curve of 0.6wt% L-threonine doped ADP shows two slopes at two different temperature range. In CBH conduction mechanism the hopping of charge carrier occurs between two defect sites over a Columbian potential barrier separating them, instead of tunnelling in potential barrier. Also, the existence of small polaron tunnelling in 0.6wt% L-threonine doped ADP may be due large degree of local lattice distortion caused by additional charge carrier such a way that the total energy like electronic and distortion of the system is thereby lowered by an amount of the polaron energy. The larger lattice distortion for 0.6wt% L-threonine doped ADP crystal can be clearly observe in powder XRD spectra.

The intrinsic defect mechanism in ADP due to L-threonine doping may be understood in following way. There will be always repulsion between two protons, each one from ADP and L-threonine, and when L-threonine donates the proton to ADP, the hydrogen of ADP is removed as a result from the bonding between $NH_4^+$ and $PO_4^{3-}$ and causes the hydrogen vacancy (L-defect) and during the course of this defect the L-threonine will combine with ADP. Hence, the doping of L-threonine by virtue of L-defect in structure of

ADP may be the appropriate reason for the change in the properties founded presently. The same mechanism was given by Govani et al. [42] for doping of L-arginine in potassium dihydrogen phosphate (KDP) crystals.

## 8. Photoconductivity study

Photoconductivity is an important property of solids by means of which the bulk conductivity of the sample changes due to incident radiation. The process of photoconduction involves generation and recombination of charge carrier and their transport to the electrodes [43]. This process takes place due to any one of the following mechanisms; band-to-band transitions, impurity levels to band edge transitions, deep level to conduction band transitions and ionization of donors [44].

Photoconductivity measurement of pure and L-threonine doped ADP crystals were made using Keithley 485 picoammeter. The (2 0 0) plane of well polished crystals having thickness of 2 mm is chosen for study. The silver paste is coated over the crystal and it ensures electrical contact between the crystal and copper electrode. The halogen lamp of power 100W and wavelength 3.17 μm is used for study. The crystal is connected in series and the dark current is recorded in the absence of any radiation and then crystals are exposed to radiation and photocurrent is recorded. The experiment is performed at room temperature and the applied field is varied from 5 to 100 V/cm.

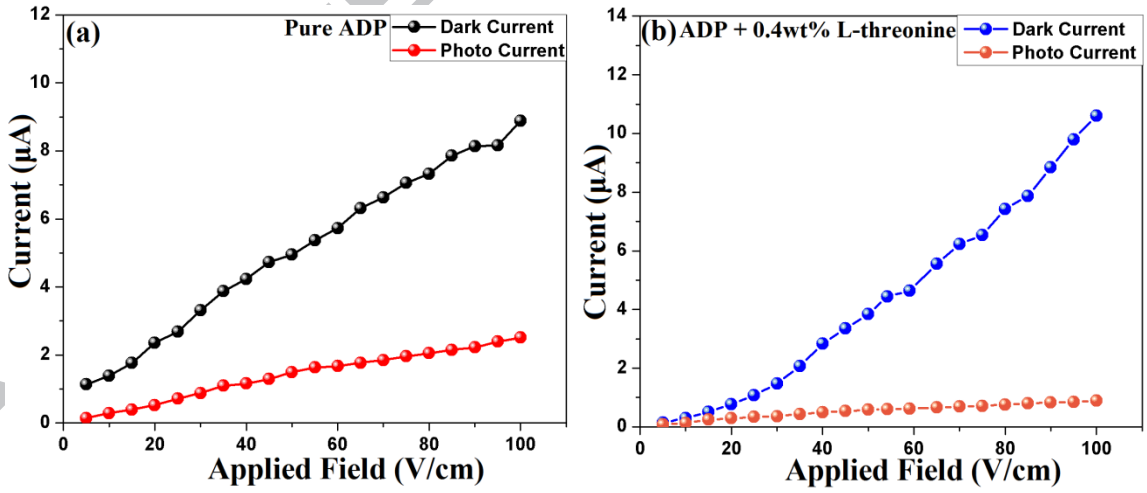

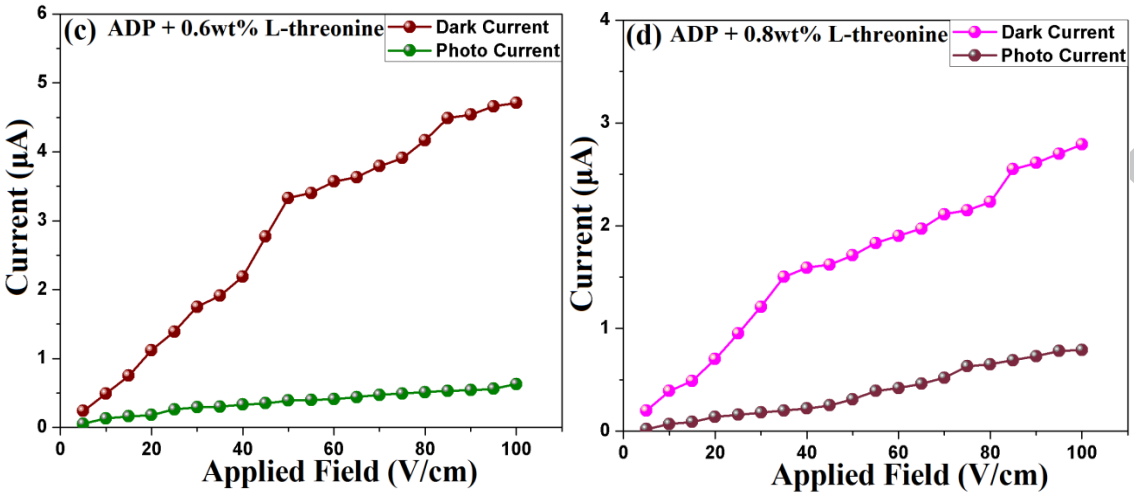


**Fig.18 (a-d)** Photoconductivity spectra of pure and L-threonine doped ADP crystal

The Figure 18 (a-d) shows the photoconductivity plots of dark and photo currents versus applied field for pure and L-threonine doped ADP crystals. From the Figures it can be seen that dark current ($I_D$) and photo current ($I_P$) increases linearly with applied field for all grown crystals. The dark current is found to be greater than photo current suggesting negative photoconductivity for all grown crystals. The negative photoconductivity attributed to the reduction in number of charge carries or their life time in the presence of radiation [45].

The negative photoconductivity can be explained on the basis of Stockmann model, according to which the forbidden gap contains two energy levels. The upper energy level is situated between the Fermi level and the conduction band, whereas the other one is located in the neighbourhood of the valence band. The lower level has high capture cross-section for electrons from the conduction band and holes from the valence band. As a result, when the sample is kept under exposed light, the recombination of electrons and holes takes place, resulting in decrease in the number of mobile charge carriers, resulting negative photoconductivity [46]. As pure and L-threonine doped ADP crystals possess negative photoconductivity they can be used for UV and IR detector applications [47].

## 9. Linear refractive index measurement

The measured linear refractive index of pure and 0.4wt%, 0.6wt% and 0.8wt% L-threonine doped ADP crystals are found to be 1.523, 1.531, 1.525 and 1.533, respectively.

The refractive indices of pure and L-threonine doped ADP crystals are measured and calculated by different techniques like optical transmittance, ordinary and extra ordinary ray refractive indices and refractive index measurement through prism coupling methods match well.

## 10. Kurtz and Perry Powder SHG efficiency measurement

The Kurtz and Parry powder technique is employed to determine the nonlinear second harmonic generation (SHG) efficiency. The fine powdered sample filled micro glass capillary is illuminated by Q-switched Nd: YAG laser of 1064 nm and the output energy of emitted green light of wavelength 532 nm are measured. The SHG efficiency of pure and different weight percentage L-threonine doped ADP is listed below.

| Sample | Output Energy (mJ) | SHG Efficiency | |
|---|---|---|---|
| | | W.R.T. Pure KDP | W.R.T. Pure ADP |
| Pure KDP | 19.5 | 1 | - |
| Pure ADP | 40.3 | 2.06 | 1 |
| 0.4 LTR | 45.4 | 2.32 | 1.12 |
| 0.6 LTR | 42.8 | 2.19 | 1.06 |
| 0.8 LTR | 44.6 | 2.28 | 1.10 |

**Table 9.** SHG efficiency of pure and L-threonine doped ADP

From Table 9 one can observe that doping of L-threonine enhances the second harmonic efficiency of ADP crystal.

Amino acids consist of a proton donating carboxy (-COOH) group and the proton accepting amino ($NH_3^+$) group. Among which the carboxy group and protonic bonds are responsible for the SHG efficiency enhancement of the parent material.

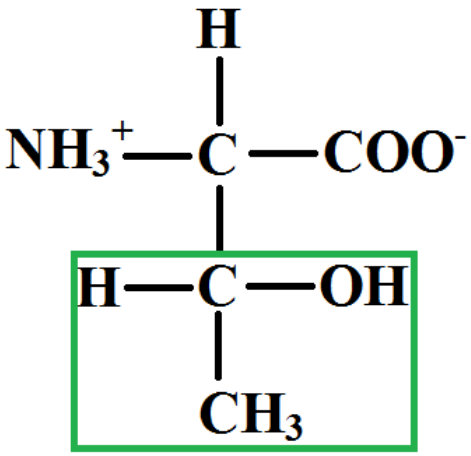


**Fig. 19.** Side chain structure of L-threonine

The Figure 19 shows side chain of L-threonine. It has a shorter side chain of hydroxy group link with carboxy group, i.e. –CH (OH) $CH_3$, due to which it is easy to remove hydrogen from the side chain of threonine and hence threonine often acts as a proton donor. During the course of threonine doping in ADP the proton and carboxy groups are introduced in structure of ADP, which ultimately increases the SHG efficiency of ADP.

For the covalent crystals like ADP, the microscopic origin of SHG enhancement may be given as follows: under the course of induced optical field, the electronic states of crystals will redistribute and the new formation of electronic states then called the ground state mixtures. This dynamic covelency will be coupled with crystal anisotropies or even phonon induced structure displacements which gives rise to large electronic polarizibility. [48-49]

## 10. Z-scan

The absolute magnitude and sign of complex third order nonlinear susceptibility ($\chi^{(3)}$) of grown crystal can be measured using Z-scan technique. The nonlinear parameters like nonlinear optical refractive index (NLR ($n_2$)) and nonlinear absorption coefficient (NLA (β)) have been determined by operating Z-scan setup in closed and opened aperture modes. Here NLR corresponds to real part of ($\chi^{(3)}$) and NLA corresponds to imaginary part of ($\chi^{(3)}$).

The difference between the peak and valley transmission ($\Delta T_{p-v}$) is written in terms of the on axis phase shift at the focus as [50],

$$\Delta T_{p-v} = 0.0406(1-S)^{0.25} |\Delta\phi| \quad (14)$$

*Where,* $|\Delta\phi|$ *= On axis phase shift*

The aperture linear transmittance (S) is calculated using the relation,

$$S = 1 - exp\,(-2r_a^2/\omega_a^2) \quad (15)$$

*Where,* $r_a$ *= The aperture,* $\omega_a$ *=The beam radius at the aperture.*

The nonlinear refractive index is give by

$$n_2 = \frac{\Delta\emptyset}{kI_0L_{eff}} \quad (16)$$

*Where, $k = 2\pi/\lambda$ = Wave vector ($\lambda$ is the wavelength of laser), $I_0$ = The intensity of the laser beam at the focus (Z=0), $L_{eff} = (1-\exp(-\alpha L)/\alpha)$ = The effective thickness of the sample, $\alpha$ = The linear absorption coefficient, L = The thickness of sample.*

The nonlinear absorption coefficient is estimated from the open aperture data using following relation,

$$\boldsymbol{\beta = \frac{2\sqrt{2}\,\Delta T}{I_0 L_{eff}}} \tag{17}$$

*Where, $\Delta T$ = The one valley value at the open aperture Z-scan curve.*

The β may be negative or positive for saturable absorption (SA) and reverse saturable absorption (RSA), respectively.

The real and imaginary parts of the third order nonlinear optical susceptibility $\chi^{(3)}$ are defined as,

$$\boldsymbol{Re\ \chi^{(3)}\ (esu) = 10^{-4}\ (\varepsilon_0 c^2 n_0^2 n_2) / \pi\ \ (m^2/W)} \tag{18}$$

$$\boldsymbol{Im\ \chi^{(3)}\ \ (esu) = 10^{-2}\ (\varepsilon_{0C}{}^2 n_0^2 \lambda\beta) / 4\pi\ (m/W)} \tag{19}$$

*Where, $\varepsilon_0$ = The permittivity of free space, C = The velocity of light in vacuum; $n_0$ = The linear refractive index.*

From the real and imaginary parts of the third order nonlinear optical susceptibility, the absolute value of $\chi^{(3)}$ can be calculated using equation,

$$\boldsymbol{\chi^{(3)} = \sqrt{(\mathrm{Re}\chi^3)^2 + (\mathrm{Im}\,\chi^3)^2}\ \ esu} \tag{20}$$

| | |
|---|---|
| Laser beam Wavelength (λ) | 632.8 nm |
| Lens focal length (f) | 30 mm |
| Optical path distance (Z) | 85 cm |
| Spot-size diameter in front of the aperture ($\omega_a$) | 3.3 mm |
| Aperture radius ($r_a$) | 2 mm |
| Incident intensity at the focus (Z = 0) | 26.50 MW/m$^2$ |

**Table 10.** Optical details of Z-scan setup

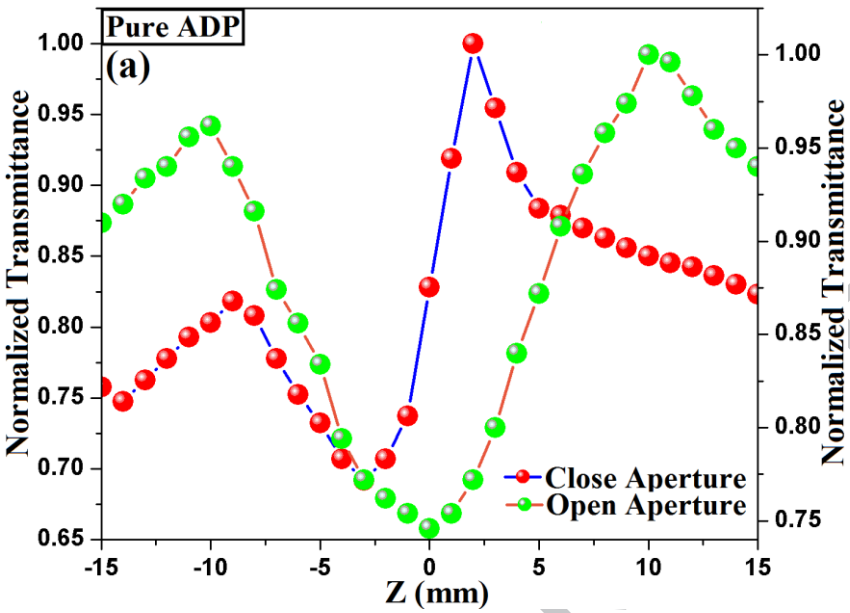


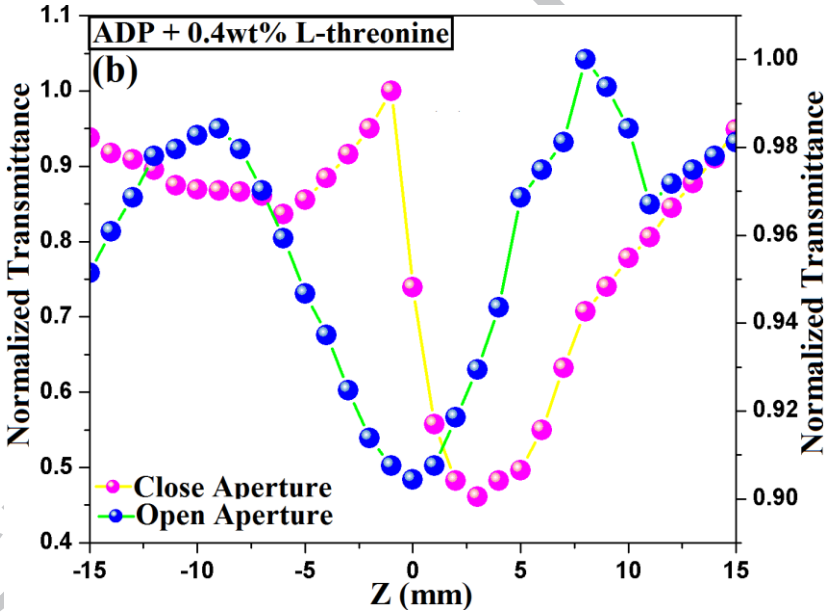


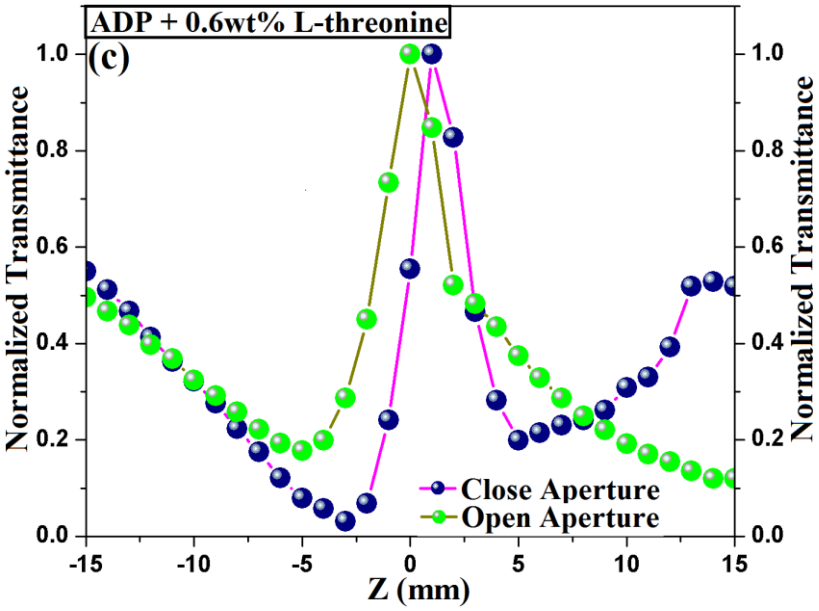

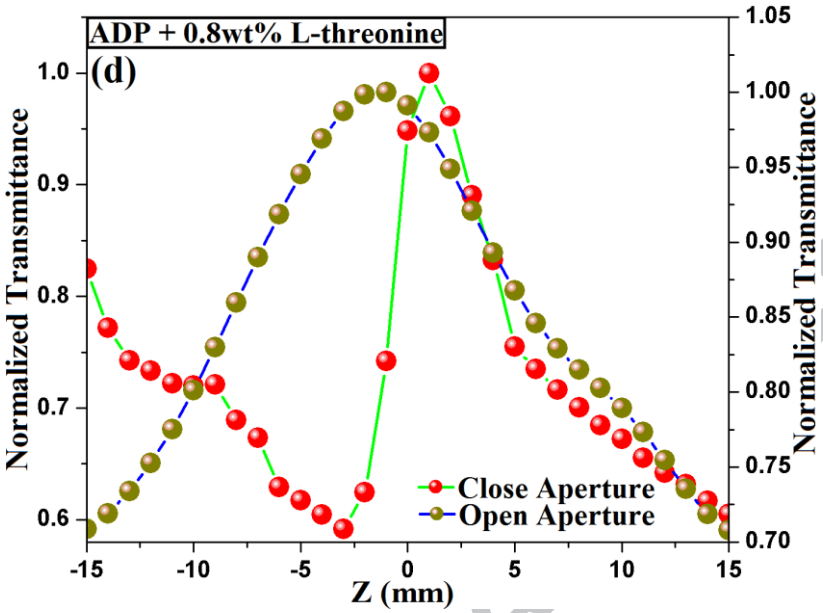


**Fig. 20(a-d)** Z-scan spectra of pure and L-threonine doped ADP crystal

The Figures 20 (a-d) shows Z-scan plots of pure and L-threonine doped ADP crystals in open and close aperture manners. The close aperture plots of pure, 0.6 wt% and 0.8 wt% L-threonine doped ADP crystals exhibit pre-focal valley and post-focal peak indicating positive nonlinear optical refractive index due to the self focusing phenomena, while the same plots of 0.4 wt% L-threonine doped ADP crystals exhibit pre-focal peak and post-focal valley indicating negative nonlinear optical refractive index due to the self defocusing phenomena. Hence, the crystals with positive nonlinear optical refractive index find applications in the optical limiting and optical switching [51-52], while the crystal with negative nonlinear optical refractive index can be utilize as night vision sensor device [53].

Usually, in the nonlinear optical medium, when the laser beam incident of crystal, if this beam remains very intends at the centre of crystals rather than edge of crystal then the crystals have positive value of $n_2$, under this circumstances, the self focusing effect occurs. In this situation the optical path length of laser beam will be greater at the centre than beam at the edge for laser. While the self defocusing in NLO crystal results due to shorter optical path length of laser beam at centre than edge of crystal, which causes negative value of $n_2$. Schematically, the self focusing and self defocusing effect in nonlinear optical medium is illustrated in Figures 21-22.

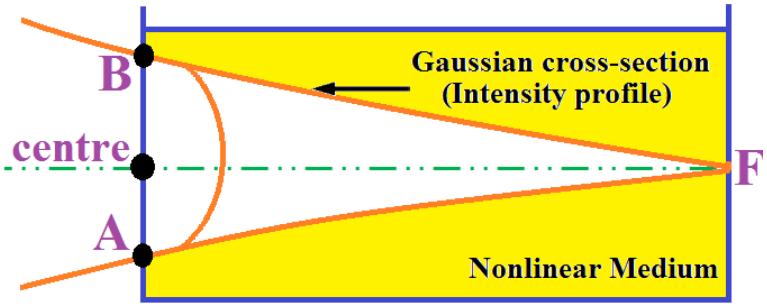


**Fig.21** Self focusing effect in nonlinear medium

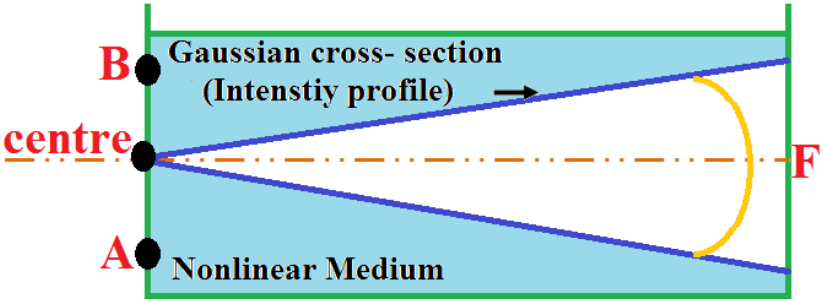


**Fig.22** Self defocusing effect in nonlinear medium

The open aperture plots of pure and 0.4wt% exhibits Reverse saturable absorption (RSA) kind of behaviour as the normalized transmittance of both samples decreases and become minimum at the focus (Z=0). The RSA is observed here due to fact that the atoms of ground and exited state absorb the photons of same wavelength in crystal. From the RSA behaviour, it may notice that the absorption increases with increase in input laser power which may be due to increment of atom population in exited state compared to loosely absorbed ground state. The RSA effect is the combination of two-photo absorption, the exited state absorption, free carrier absorption and nonlinear scatting etc. [54-55].

To excite a molecule from ground state to high energy electronic state, if the two photon of identical or different frequency absorbed at same time then the two photon absorption process occurs. It is a third order nonlinear optical process because it is directly related to the imaginary part of third order susceptibility ($\chi^{(3)}$) and such process depends on the square of incident light intensity.

The open aperture plots of 0.6 wt% and 0.8 wt% show that the normalized transmittance increases with the increase in input laser power suggesting the Saturable absorption (SA) phenomena in both crystals. The saturable absorption process in crystal is describe as, when the highly intense laser beam is incident on ground state atoms, they absorb the photons and transit to the exited state at such a rate that there will be insufficient

time for them to return back to the ground state before the ground state becomes depleted and the absorption of photons by atoms subsequently get saturated.

The third order nonlinear optical susceptibilities of pure and L-threonine doped ADP crystals are compiled in table 11. From that table it can be seen that, the $\chi^{(3)}$ increases for 0.4 wt% and 0.8 wt% L-threonine doped ADP crystals compare d to pure ADP, whereas the same decreases for 0.6 wt% L-threonine doped ADP crystal.

Although, the obtained values of third order susceptibilities of pure and L-threonine doped ADP are compared with other potential NLO crystals of KDP family and other organic crystals [28][56-57] and it is found that the present pure and doped crystals have higher third order susceptibilities compared to the available values in the literature for other crystals.

| Sample | $\Delta T_{p-v}$ | $n_2$ ($cm^2$ / W) | β (cm / W) | $\chi^{(3)}$ (esu) |
|---|---|---|---|---|
| Pure ADP | 0.00196 | $6.34 \times 10^{-11}$ | $9.55 \times 10^{-6}$ | $1.73939 \times 10^{-5}$ |
| ADP + 0.4wt% L-threonine | 0.00344 | $- 9.24 \times 10^{-11}$ | $9.62 \times 10^{-6}$ | $1.88365 \times 10^{-5}$ |
| ADP + 0.6wt% L-threonine | 0.00617 | $1.79 \times 10^{-10}$ | $2.04 \times 10^{-6}$ | $4.11553 \times 10^{-6}$ |
| ADP + 0.8wt% L-threonine | 0.0026 | $8.44 \times 10^{-11}$ | $9.10 \times 10^{-6}$ | $1.78382 \times 10^{-5}$ |

**Table 11.** Z-scan parameters of pure and L-threonine doped ADP crystal

Here one may notice that the 0.4wt% L-threonine doped ADP crystal has highest magnitude of third order susceptibility among the other which may due to result of enhanced delocalization of conjugated π-electron cloud that makes molecule highly polarized [58].The decrement of third order susceptibility in the case of 0.6 wt% L-threonine doped ADP may be due to the fact that when the addition of charge carrier to localized sites of crystal matrix causes the large degree of local lattice distortion, the hydrogen bonding network of ADP may gets disturbed at the larger extend which ultimately, diminishes the nonlinear optical properties of the crystal.

## 11. Laser threshold damage (LDT) study

The laser threshold damage (LDT) of NLO crystal is defined as a measure of crystal surface damage under the influence of high-power laser beam. This study involves the optical processes like electron avalanche, multi photon absorption and photo ionization for NLO crystals . Further, the damage of crystal surface by laser reflects the crystalline imperfection like growth sector boundaries, dislocations of crystal [59].

Presently, the LDT study of pure and L-threonine doped ADP crystals have been carried using Q-switched Nd: YAG pulsed laser of wavelength of 1064 nm. The laser beam was operated in $TM_{00}$ mode with pulse width of 10 ns and the repetition frequency rate of 10 Hz. By using the variable attenuator, the output power of incident laser beam of 1 mm diameter could be controlled. This beam was incident on crystal placed at the focus of the converging lens of focal length 30 cm. The power meter was placed to determine the energy density of input laser beam when the crystal gets damage.

The power density ($P_d$) was calculated using the relation,

$$P_d = \frac{E}{\tau \pi r} \quad (21)$$

*Where, E = Input energy density (mJ), τ = Pulse width (ns) and r = Area of the circular spot (mm).*

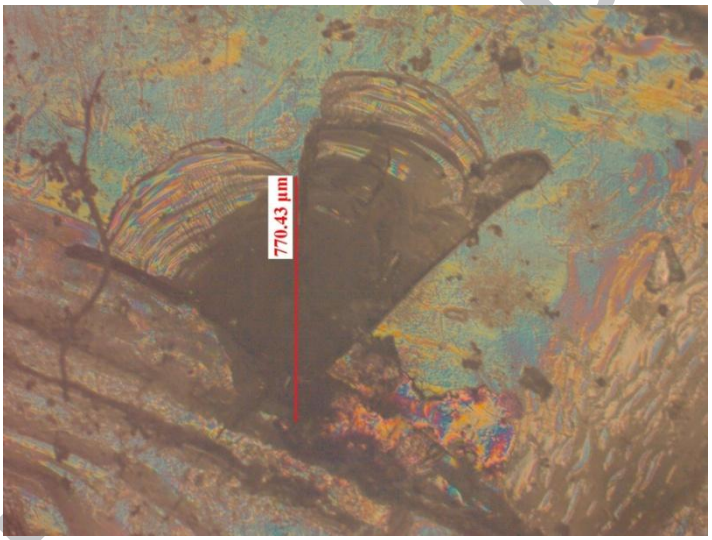


**Fig. 23** laser threshold damage spot of ADP + 0.6wt% L-threonine crystal

The calculated values of laser threshold damage for pure and L-threonine doped ADP crystals are tabulated in table 12.

| Sample | Power density ($P_d$) (GW / $cm^2$) |
|---|---|
| Pure ADP | 3.55 |
| ADP + 0.4wt% L-threonine | 9.94 |
| ADP + 0.6wt% L-threonine | 5.98 |
| ADP + 0.8wt% L-threonine | 1.70 |

**Table 12.** Power density values of pure and L-threonine doped ADP crystals

From the table it can be observed that the 0.4wt% L-threonine doped ADP sample has the higher LDT among the other crystals, which may due to highest crystalline perfection, highest molecular chirality and polarizibility, free from growth sector boundary. This result is supported by other nonlinear optical

measurements like second and third harmonic generation efficiency. Beside this the obtained value of LDT for pure and doped ADP samples are quite higher than various inorganic and organic NLO crystals available in the literature [60-61].

## Conclusions

The pure and different weight percentage L-threonine doped ADP crystals were successfully grown. The Powder XRD study suggested single phase nature, lattice strain and defect caused by dopant in ADP. The FT-IR spectra confirmed the presence of all constitute functional group of ADP. The FT-Raman spectra have shown various normal modes of vibration for $NH_4^+$ and $PO_4^{3-}$ group and suggested that the dopant retained original $PO_4^{3-}$ framework in ADP. The PL emission spectra of pure and doped ADP have shown recombination of electron (L-defect) and hole (D-defect) at different photon energies. The presence of Stoke shift and vibration relaxation phenomena confirmed the defect in ADP due to doping. The CHN analysis confirmed presence of dopant in ADP. The UV-Visible spectroscopy suggested increment in transmittance, energy band gap and skin depth due to doping in ADP. The Wemple-DiDomenico single oscillator model confirmed existence of dopant in ADP by means of decreased single oscillator energy for doped ADP. The presence of thermally activated charge carrier was suggested by capacitance study and the conductance curve suggested CBH and NSPT kind of conduction mechanism for pure and doped ADP occurred due to increase of unoccupied hydrogen vacancies in ADP. The linear refractive indices of pure and doped ADP showed harmony with each other as measured by different technique like transmittance spectra, prism coupling method. The uniaxial negative crystal nature of ADP was suggested by ordinary and extra ordinary refractive index calculation. The nonlinear optical properties were improved due to doping of L-threonine in ADP as shown by SHG, Z-scan and LDT studies.

Ultimately, the doping of L-threonine improved the linear and nonlinear optical performance of ADP crystals and the central theme suggested that the doped crystals are prominent candidates for various NLO applications.

## Acknowledgement

The authors are thankful to UGC, New Delhi, for funding under DRS-SAP and DST, New Delhi, for FIST. The authors also acknowledge the encouragement and keen interest from H.O.D. Physics, Saurashtra University, Rajkot and M.S. University of Baroda, Vadodara. One of the authors (JHJ) is highly thankful to Department of Education, Government of Gujarat to allow him to carry out research activity. The author (JHJ) is sincerely

thankful to Dr. K.V.R. Moorthy (Department of Applied Physics, M.S.University of Baroda) for Photoluminescence spectroscopy and Dr. P.Sagayaraj (Department of Physics, Loyala College, Chennai) for Photoconductivity study.

## References

[1] C.Sun and D.Xue, Crystalline behavior of KDP and ADP crystals, Opt.Mat.,36(2014)1966-1969.doi:10.1016/j.optmat.2013.12.019.

[2] L.N.Rashkovich, KDP-Family Single Crystals, Hilger, Bristol, 1991.

[3] A.Puhal Raj, C.Ramachandra Raja, Synthesis, Growth, Structural, Spectroscopic, Thermal and Optical Propertiesof NLO Single Crystal: L-Threonine Zinc Acetate, Photon. & Optoelect. 2(3)(2013) 56-64.

[4] Parikh K.D., Dave D.J., Joshi M.J., Growth and characterization of L-alanine doped KDP crystals, Crystal Res. & Technol. 45 (2010) 603-610.

[5] K. D. Parikh, D. J. Dave, B. B. Parekh, M. J. Joshi, Thermal, FT-IR and SHG efficiency studies of L-arginine doped KDP crystals, Bull. Mater. Sci. 30 (2007) 105-112.

[6] Parikh K. D., Dave D.J., Joshi M.J., Crystal growth, thermal, optical and dielectric properties of L-lysine doped KDP crystals, Modern Physics Letters B, 23, (2009) 1589-1602.

[7] Hasmuddin M., Singh P., Shkir M., Abdullah M.M., Vijayan N., Bhagavannarayana G., Wahab M.A., Structural, spectroscopic, optical, dielectric and mechanical study of pure and L-proline doped ammonium dihydrogen phosphate single crystals, Spectchim.Acta. A, 123(2014)376-384.

[8] Janczak J., Zobel D., Luger P., *L-threonine at 12 K*, Acta Crystallographica C, 53(1997)1901-1904.

[9] Dave D. J., Parikh K. D., Parekh B. B., Joshi M. J., Growth and Spectroscopic, Thermal, Dielectric and SHG studies of L- Threonine Doped KDP Crystals, J.Optoelec. Adv. Mater., 11 (2009) 602.

[10] Rajesh P., Ramasamy P., Mahadevan C.K., Effect of L-lysine monohydrochloride dihydrate on the growth and properties of ammonium dihydrogen orthophosphate single crystals, J.Cryt.Grow., 311(2009)1156-1160.

[11]Xu, D.; Xue, D., Chemical bond analysis of the crystal growth of KDO and ADP, J.Cryt.Grow.,286(2006) 108-113.

[12] Hasmuddin M., Singh P., Sakir M., Abdullah M.M., Vijayan N., Ganehs V., Wahab M.A., Study of pure and l-tartaric acid doped ammonium dihydrogen phosphate single crystals: A novel nonlinear optical non-centrosymmetric crystal, Mat.Chem.Phys., 144(2014)293-300.

[13] Colthup N.B., Daly L.H., Wiberley S.E., Introduction to Infrared and Raman Spectroscopy, 3rd ed. Academic press;1975.

[14] Joshi V.S., Joshi M.J., FT-IR spectroscopic and thermal studies of calcium tartrate trihydrate crystals grown by gel assistance. Ind.J.Phy.,75(2001)159-163.

[15] F. Ben Brahim, A. Bulou, Growth and spectroscopy studies of ADP single crystals with l-glutamine and l-cysteine amino acids Vibra.Tech.,65 (2013) 176– 185.

[16] F. Ben Brahim, A.Bulou, Growth and spectroscopy studies of ADP single crystals with l-proline and l-arginine amino acids Mater.Chem.Phys.,130 (2011) 24– 32.

[17] Gfroerer T.H., *Photoluminescence in analysis of surfaces and interfaces Encyclopedia of Analytical Chemistry*, John Wiley & Sons Ltd. Chichester, pp. 9209-9231.

[18] Portia S.A.U., Jayanthi K., Ramamoorthy K., Growth and Characterization of Pure and Disodium Hydrogen Phosphate mixed with Potassium Dihydrogen Phosphate Crystal by using slow evaporation technique, Amr.J.Bio.Pharm.Res., 1(2)(2014)77-82.

[19] Gispert J.R., Coordination chemistry, Wiley- VCH, 2008 pp.483.

[20] Kitai A., Luminescent Material and Application, Wiley, p.32.

[21] Hiroshi F., Straub J.E., Vibrational energy relaxation in proteins, PNAS, 102(2005)6726-6731.

[22] Takmakoff A., Lecture notes on vibrational relaxation, MIT Department of Chemistry.

[23] Ogorodnikova I.N., Kirm, M., Pustovarov V.A., Luminescence of the hydrogen bonded crystals, Radia.Meas., 42(2007)746-750.

[24] Voronov A.P., Salo V.I., Puzikov M., Tkachenko V.F., Vydaoe Y.T., Potassium and Ammonium Dihydrogen Phosphates Activated with Thallium: Growth and Luminescence and Scintillation Properties, Cryst.Rep., 51(2006) 696-701.

[25] Parthasarathy M., Ananthraja M., Gopalkrishnan R., Growth and characterization of large single crystal of L-serine methyl ester hydrocholoride, J.Cryt.Grow., 340(2012)118.

[26] Akhtar F., Podder J., Structural, Optical, Electrical and Thermal Characterizations of Pure and L-alanine Doped Ammonium Dihydrogen Phosphate Crystals, J.Crytl.Proc.Tech., 1(2011)18-25.

[27] Shaikh R.N., Anis M., Shirsat M.D., Hussaini S.S., Study on optical properties of L-valine doped ADP crystal, Spect.Chimi.Acta A.,136 (2015) 1243‑1248.

[28] Shaikh R.N., Shirsat M.D., Koinkar P.M., Hussaini S.S., Effect of L-cysteine on optical,thermal and mechanical properties of ADP crystal for NLO application, Opt.Las.Tech., 69(2015)8-1.

[29] Shaikh R.N., Anis M., Shirsat M.D., Hussain S.S., Investigation on the Linear and Nonlinear Optical Properties of L-Lysine Doped Ammonium Dihydrogen Phosphate Crystal for NLO Applications, J.Appl.Phys., 6(2014)42-46.

[30] Shaikh R.N., Mitkar S.R., Anis M., Shirsat M.D., Hussain S.S., Optical Studies of Amino acids doped Ammonium Dihydrogen Phosphate (ADP) crystals for NLO Applications, Int.J.Chemtech.Res., 6(2014)1617-1620.

[31] Bakr N.A., Funde A.M., Waman V.S., Kamble M.M., Hawaldar R.R., Amalnerkar D.P., Gosavi S.W., Jadkar S.R., Determination of the optical parameters of a-Si:H thin films deposited by hot wire–chemical vapour deposition technique using transmission spectrum only, Pramana, 6(2011)519-531.

[32]Girisun C.S., Dhanuskodi S., Linear and nonlinear optical properties of tris tihourea zince sulphate single crystals. Crysta.Res.Tech., 44(2009)1297.

[33] Allred A.L., Electronnegativity value from thermochemical data, J. Inorg. Nucl. Chem. 1 (1961) 215.

[34] Wemple S.H., DiDomenico M.Jr., Behaviour of Electronic Dielectric Constant in Covalent and Ionic Materials. Phy.Rev.B.,3(4) (1971) 1338-50.

[35] Farag A.A.M., Rafea M.A., Roushdy N., El-Shazly O., El-Wahidy E.F., Influence of Cd-content on structural and optical dispersion characteristics of nanocrsytalline $Zn_{1-x}Cd_xS$ films.J.Alloy.Compd.,621(2015)434-40.

[36] Biecerano J., Ovshinesky S.R., Chemical bond approch to the structure of chalcogenide glasses with reversible switching properties, J.Non Cryst.Solids, 74(1985)75.

[37] Ertugrul R., Tataroglu A., Influence of Temperature and Frequency on Dielectric Permittivity and ac Conductivity of Au/SnO2/n-Si (MOS) Structures Chin.Phys.Lett., 29(2012)077304.

[38] Ataseven T., Tataroglu A., Temperature-dependent dielectric properties of Au/Si3N4/n-Si (metal insulator semiconductor) structure Chin.Phys.Lett.,22(2013)117310.

[39] Haung J.P., Yu K.W., New Nonlinear Optial Materials: Theoretical Research, Nova publication.

[40] Meena M., Mahadevan C.K., Growth and electrical characterization of L-arginine added KDP and ADP Single crystals. Cryst.Res.Tech.,43(2008)166-172.

[41] Joshi J.H., Kanchan D.K., Joshi M.J., Jethva H.O., Parikh K.D., Dielectric relaxation, complex impedance and modulus spectroscopic studies of mix phase rod like cobalt sulfide nanoparticles, Mat.Res.Bull., 93 (2017) 63–73.

[42] Govani J.R., Durrer W.G., Manciu M., Botez C., Manciu F.S., Spectroscopic study of L-arginine interaction with potassium dihydrogen phosphate crystals, J.Mater.Res., 24(2009)2316-2320.

[43] Rajkumar M.A., Stanly John Xavier S., Anbarasu S., Devarajan P.A., Microhardness, dielectric and photoconductivity studies of 2-Amino 5-Nitro pyridinium nitrate NLO single crystals, Res. J. Phy.Sci. 2(2014)1-4.

[44] Bincy I.P., Gopalakrishnan R., Synthesis, growth and characterization of new organic crystal: 2-Aminopyridinium p-Toluenesulfonate for third order nonlinear optical applications, J.Crysta.Growth, 402(2014)22.

[45] Bube R.H., Photoconductivity of solids, Wiley, 1981.

[46] Sagadevan S., Varatharajan R., Studies on the growth and microhardness, dielectric and photoconductivity of NLO material Ammonium acid phthalate, Int.J.Comp.App., 75(2013)28-32.

[47] Joshi V.N., Photoconductivity, Marcel Dekker, 1990.

[48] Reshak A.H., Kityk I.V., Auluck S., Investigation of the Linear and Nonlinear Optical Susceptibilities of KTiOPO4 Single Crystals: Theory and Experiment, J.Phys.Chem., 114(2010)16705-16712.

[49] Stucky G.D., Philips M.L.F., Gier T.E., The Potassium Titanyl Phosphate Structure Field: A Model for New Nonlinear Optical Materials, Chem.Meter., 1(1989)492-509.

[50] Senthil K., Kalainathan S., Ruban Kumar A., Arvinan P.G., Investigation on synthesis, crystal structure and third-order NLO properties of a newstilbazolium derivative crystal: A promising material for nonlinear optical devices, RSC advances, 2014.

[51] Ashok Kumar R., Ezhil Vizhi R., Vijayan N., Bhagavannarayanan G., Rajan Babu D., Growth, Crystalline Perfection and Z-scan Studies of Nonlinear Optical alpha-Lithium Iodate Single Crystal, J.Pure Appl. & Ind.Phys., 1(1)(2010)61-67.

[52] Natarajan V., Sivanesan T., Pandi S., Third order non-linear optical properties of potassium aluminium sulphate single crystals by Z-scan technique, Ind. J. Sci. Technol. 3(2010)656-658.

[53] Dhanaraj P.V., Rajesh N.P., Investigations on crystal growth, structural, optical, dielectric, mechanical and thermal properties of a novel optical crystal: nicotinium nitrate monohydrate, J. Crys. Grow., 318(2011) 974–978.

[54] Nagarajan K.K., Pramodini S., Santhoskumar A., Nagaraja H.S., Poornesh P., Kekuda D., Third order nonlinear optical properties of Mn doped ZnO thin films under CW illumination, Opt.Mater., 35(2013)431-439.

[55] Frobel P.G.L., Suresh S.R., Mayadevi S., Sreeja S., Mukherjee C., Muneera C.I., Intense low threshold nonlinear absorption and nonlinear refraction in a new organic polymer nanocomposite, Mater.Chem.Phys., 129(2011)981-989.

[56] Anis M., Shirsat M.D., Muley G., Hussaini S.S., Influence of formic acid on electrical, linear and nonlinear optical properties of potassium dihydrogen phosphate (KDP) crystals, Physica B, 449(2014)61-66.

[57] Selvakumar S., Boobalan M.S., Babu S.A., Ramalingam S., Rajesh A.L., Crystal growth and DFT insight on sodium para-nitrophenolate para-nitrophenol dihydrate single crystal for NLO application, J.Mole.Stru., 1125(2016)1-11.

[58] Anis M., Shirsat M.D., Muley G., Hussaini S.S., Influence of formic acid on electrical, linear and nonlinear optical properties of potassium dihydrogen phosphate (KDP) crystals, Phys.B., 449(2014)61-66.

[59] Alexandru H.V., Antohe S., Prismatic face of KDP crystal, kinetic and mechanism of growth from solution, J.Crys. Grow., 258(2003)149-157.

[60] Rajesh P., Sreedhar S., Boopathi K., Venugopal Rao S., Ramansamy P., Enhancement of the crystalline perfection of <0 0 1> directed KDP single crystal, Curr.appl.phys., 11(2011)1343-1348.

[61] Rajkumar M., Chandramohan A., Synthesis, growth, characterisation and laser damage threshold studies of N,N-dimethylanilinium-3-carboxy-4- hydroxybenzenesulphonate crystal: An efficient SHG material for electro-optic applications, Opt.Mater., 66(2017)261-270.